

**Quantification of Uranium and Thorium at Cheptais Anomaly Using Energy
Dispersive X-Ray Fluorescence Method for Mineral Content and Evaluation of
Associated Radio-ecological Hazards**

Kenneth Anakoli (BSc, Geology)


A thesis submitted in partial fulfillment for the requirements for the award of degree of
Master of Science in Nuclear Science of the University of Nairobi

August 2020

DECLARATION

I hereby declare that this thesis is my original work and has not been submitted for the award of any degree or qualification at any other University.

Kenneth Andibo Anakoli, S56/78206/2015

Signature.......... Date 12th August, 2020.....

Supervisors' approval

This thesis has been submitted with our knowledge and approval as university supervisors:

- 1) Mr Michael J. Mangala,
Institute of Nuclear Science and Technology,
University of Nairobi

Signature.......... Date 12/8/2020.....

- 2) Dr. Zachariah N. Kuria,
Department of Geology,
University of Nairobi

Signature.......... Date 12th AUGUST 2020.....

DEDICATION

To my father, the late Elsaphane Odinga Anakoli.

ACKNOWLEDGEMENT

I would like to thank the Nuclear Power and Energy Agency (NuPEA), for giving me time to study, despite the enormous workload that I left behind, during my entire study period; the Institute of Nuclear Science and Technology community, University of Nairobi, for their support during my entire period of study.

I thank my supervisors; Mr Michael Mangala, Lecturer, Institute of Nuclear Science & Technology, University of Nairobi and Dr Zachariah Kuria, Lecturer, Department of Geology, University of Nairobi for guiding me throughout my research and Mr Emmanuel Mulehane, geologist at NuPEA for helping me out with the development of the maps.

And finally, to God for mental and spiritual guidance throughout the process of writing this thesis.

ABSTRACT

The economies of most developing countries, largely depends on a stable and abundant supply of mineral resources and affordable energy supply. Following an airborne radiometric survey in the country, by the Department of Mines and Geology, a number of radioactive anomalies were delineated, in areas such as Chesikaki, Masaba and Cheptais. However, ground follow up surveys have not been conducted to determine the spatial distribution and the extent of occurrence of these minerals to date. This study was conducted in Cheptais area of Mt. Elgon region, specifically, to determine thorium-232 and uranium-238 radioactivity levels and to estimate the radiological hazard indices associated with these radionuclides. The study also determined the elemental content distribution of other potential minerals for economic development and the associated radiation hazard indices. The radiometric survey was done using an ionizing radiation meter, RSKB-104 to measure gamma radiation field equivalent dose rate in the sampled areas. Five readings were recorded at each sampled site. A heat map was then generated from the radiometric measurements to show the variation of background radiation levels. In addition, a total of thirty-six (36) soil samples and seven (7) rock samples were evaluated for mineral elements contents, using AMPTEK Experimenters' Kit Energy Dispersive X-ray Fluorescence Spectrometer. Prior to measurements, these samples were crushed, homogenized and left to achieve secular equilibrium for approximately two months. The results of elemental content analysis indicate, two major constituents in the soil samples; potassium(K) and iron(Fe) recorded mean concentration 15,498 $\mu\text{g/g}$ (1,972 $\mu\text{g/g}$ – 289,800 $\mu\text{g/g}$) and 116,457 $\mu\text{g/g}$ (236 $\mu\text{g/g}$ – 37,166 $\mu\text{g/g}$), respectively. The other trace constituents include; manganese, copper, zinc, lead, uranium and thorium. From the activity concentration measurements, it was established that, ^{40}K was the greatest contributor to radiation exposure with a mean activity concentration of $553 \pm 11 \text{ Bq kg}^{-1}$ (65.5%), ^{232}Th and ^{238}U at 215 Bq kg^{-1} (25.4%) and 76 Bq kg^{-1} (9.1%), respectively and all, exceed the UNSCEAR global mean of 400, 30 and 35 Bq kg^{-1} respectively. The radium equivalent values ranged between 32 – 1401 Bq kg^{-1} , with a mean of 425.91 Bq kg^{-1} ; which is significantly higher than the world average of 160 Bq kg^{-1} and the UNSCEAR permissible limit of 350 Bq kg^{-1} . In addition, associated radiation hazards indices; gamma radiation index, I_{yr} , the external

hazard index, H_{ex} and the internal hazard index, H_{in} , were determined to be 3.03, 1.15 and 1.36, respectively, all exceeded the required index of unity (≤ 1).

The results of the statistical data analysis indicate a weak positive correlation between uranium-238 and potassium-40 ($R^2=0.1692$) and between uranium-238 and thorium-232 ($R^2=0.52$). However, there was a negative correlation between thorium-232 and potassium-40 ($R^2= - 0.1805$). There is a significant difference in the variation of activity concentration levels between each of the naturally occurring radio nuclides; ^{232}Th and ^{238}U , ^{238}U and ^{40}K and ^{232}Th and ^{40}K . The absorbed dose rates (DR) due to gamma radiations in air, 1 m above the ground, was determined to have a mean of 198.5 nGy/h and exceeds the world average of 57 nGy/h. The annual effective dose with an outdoor occupancy factor of 0.4, assumed, had a mean value of 0.48 mSv/y, and is below the worldwide mean annual effective dose of 0.5 mSv yr⁻¹. In conclusion, the radioactivity levels in most parts of Cheptais area of Mt. Elgon region in Bungoma County, currently, do not pose health risks to the public. However, the central part of the study area requires further studies to ascertain the level of risks posed by elevated background radiation readings that were recorded in the study area. This study complements the existing pool of knowledge in the area of mineral explorations and radio-ecological studies in the country.

LIST OF ABBREVIATIONS

AEDE	Annual Effective Dose Equivalent
AXIL	Analysis of X-Ray by Iterative Least-square fitting
BGS	British Geological Survey
EDXRF	Energy Dispersive X-Ray Fluorescence
ENS	European Nuclear Society
EPRI	Electric Power Research Institute
GPS	Global Positioning System
HPGe	High Purity Germanium detector
IAEA	International Atomic Energy Agency
ICRP	International Commission on Radiation Protection
INST	Institute of Nuclear Science and Technology
ME&MD	Ministry of Energy & Mineral Development
NCRP	National Council on Radiation Protection
NEI	Nuclear Energy Institute
NORM	Naturally Occurring Radioactive Materials
OECD	Organization for Economic Cooperation and Development
PTXRF	Proficiency Test for X-Ray Fluorescence
QXAS	Quantitative X-Ray Analysis System
Ra _{eq}	Radium equivalent
REE	Rare Earth Elements
TENORM	Technologically Enhanced Naturally Occurring Radioactive Materials
UNSCEAR	United Nations Scientific Committee on the Effects of Atomic Radiation
US-EPA	United States Environmental Protection Agency
WNA	World Nuclear Association
WNO	World Nuclear Organization
XRD	X-Ray Diffraction
XRF	X-Ray Fluorescence

TABLE OF CONTENTS

DECLARATION **Error! Bookmark not defined.**

DEDICATION ii

ACKNOWLEDGEMENT iv

ABSTRACT v

LIST OF ABBREVIATIONS vii

TABLE OF CONTENTS viii

LIST OF FIGURES xi

LIST OF TABLES xii

CHAPTER ONE: INTRODUCTION 1

 1.1 Introduction 1

 1.2 Background information 1

 1.3 Economic benefits of mining uranium 2

 1.4 Occurrence of uranium and thorium minerals 3

 1.6 The Geology of Cheptais 6

 1.7 Problem statement 6

 1.8 Objectives of the research 7

 1.8.1 General objective 7

 1.8.2 Specific objectives 8

 1.9 Justification and Scope of the Study 8

CHAPTER 2: LITERATURE REVIEW 10

 2.1 Introduction 10

 2.2 Geology and mineral occurrence in Kenya 10

 2.3 Exploration of Uranium and Thorium in Kenya 14

 2.4 Studies on Radiometric Surveys 17

CHAPTER 3: METHODOLOGY	23
3.1 Introduction	23
3.2 Description of study area	23
3.3 Field Sampling and Measurement.....	25
3.3.1 Radiometric Survey Measurements	25
3.3.2 Soil Sampling for Mineral Content Analysis and Radioactivity Measurement	26
3.4 Sample preparation for EDXRF analyses	27
3.5 Sample Preparation for Radiometric Analysis	28
3.6 Determination of Elemental Content and Radioactivity Concentrations	28
3.6.1 EDXRF Technique for Elemental Content Analysis	28
3.6.2 HpGe Gamma Spectroscopy for Radioactivity Measurements	30
3.7 Determination of Radiological Radiation Hazard Indices	34
3.7.1 Radium Equivalent Activity, gamma index, external and internal hazard indexes	34
3.7.2 Absorbed dose.....	35
3.7.3 Annual Effective Dose	35
3.8 Statistical Data Analysis	35
CHAPTER FOUR: RESULTS AND DISCUSSIONS	37
4.1 Introduction	37
4.2 Quality Assurance of EDXRF Analytical Results	37
4.3 Results of Field Measurement: Background radiation levels in the study area	38
4.4 Elemental Distribution in Soils	42
4.5 Variation of the NORMs in the soils and rock samples.....	47
4.6 Results of statistical data analysis of radioactivity	51
4.7 Radiation Hazard Indices	54

CHAPTER 5: CONCLUSION AND RECOMMENDATIONS	57
5.1 Conclusion.....	57
5.2 Recommendations	58
REFERENCES.....	59
APPENDIX I: Elemental concentrations in $\mu\text{g/g}$ in the soil samples of Cheptais area....	64

LIST OF FIGURES

Figure 2- 1: Geological map of Cheptais area	11
Figure 3- 1: Meteorological data of Cheptais area.....	24
Figure 3- 2: Map of the sampled sites within Cheptais area.....	27
Figure 3- 3: Schematic diagram of the operating principle of EDXRF.....	29
Figure 3- 4: EDXRF instrument at the INST, University of Nairobi.....	30
Figure 3- 5: HpGe instrument at INST, University of Nairobi.....	31
Figure 4- 1: Distribution of background radiation in the sampled sites.....	40
Figure 4- 2: Heat map of the study area showing the variation of background radiation levels.....	41
Figure 4- 3: Variation of concentrations of potassium-40.....	42
Figure 4- 4: Variation of concentrations of Manganese.....	43
Figure 4- 5: Variation of concentrations of iron.....	43
Figure 4- 6: Variation of concentrations of zinc.....	44
Figure 4- 7: Variation of concentrations of copper.....	44
Figure 4- 8: Variation of concentrations of lead.....	45
Figure 4- 9: Variation of concentrations of thorium-232.....	45
Figure 4- 10: Variation of concentrations of uranium-238.....	46
Figure 4- 11: HpGe Gamma Ray Spectrum of activity concentration of soils in the study area.....	48
Figure 4- 12: Variation of uranium-238, thorium-232 and potassium-40 activities in the soil samples.....	48
Figure 4- 13: Relative abundance of the naturally occurring radionuclides in the measured soil samples.....	51
Figure 4- 14: Correlation of thorium-232 with uranium -238.....	52
Figure 4- 15: Correlation of uranium-238 and potassium-40.....	53
Figure 4- 16: Correlation of thorium-232 and potassium-40.....	54

LIST OF TABLES

Table 2- 1: Value of mineral production in Kenya	13
Table 3- 1: IAEA-RGK-1: Certified reference material activity concentration (Bqkg-1)	32
Table 3- 2: Recommended energy lines for gamma-ray emitters of environmental samples.....	33
Table 4- 1: Results of Analyses of Standard Reference Material, IAEA-PTXRF-09.....	38
Table 4- 2: Survey meter measurements, n=5, $\mu \pm 1SD$	39
Table 4- 3: Minimum economic viability of ores of the elements analyzed ($\mu\text{g/g}$).....	47
Table 4- 4: Measured activity concentration of ^{232}Th , ^{238}U and ^{40}K in Bq/kg in soils; (n=1, $x \pm 1\delta$).....	49
Table 4- 5: Correlation of uranium-238, thorium-232 and potassium-40 activities.....	52
Table 4- 6: Summary of mean radiation hazard indices.....	55

CHAPTER ONE: INTRODUCTION

1.1 Introduction

The following sections in this chapter describes; the background of the research and the problem statement, the objectives of the study, the significance of the study and the justification. In addition, there is a section that discusses the scope of the research, economic benefits of mining uranium; occurrence of uranium and thorium minerals and description of the study area, its geology and on radio-ecological hazards associated with mining of uranium and thorium minerals.

In general, this study builds and contributes to the existing pool of studies in the area of mineral exploration in Kenya.

1.2 Background information

Uranium is an important nuclear fuel for all the currently operating nuclear power plants globally, and is also used in research reactors and to power submarines and in the manufacture of nuclear weapons. The earth's crust is composed of 2.7 $\mu\text{g/g}$ of natural uranium, while the oceans contain approximately 0.003 $\mu\text{g/g}$ of Uranium. Uranium occurs naturally in various mineral ores, which include uraninite, also known as pitchblende ($\text{U}_2\text{O}_5 \cdot \text{UO}_3$ or U_3O_8), and in range of other ores such as carbonitite and davidite (Nash, 2010).

Worldwide, uranium mines are located in twenty countries. Most of these mines have ore deposits that, average grades in excess of 1000 $\mu\text{g/g}$ (BGS, 2004). Nonetheless, some Canadian mines recorded high amounts of the uranium ores globally.

Thorium is also another potential source of nuclear fuel. Various studies have demonstrated that nuclear reactors can be designed to use thorium-232 to power them for production of electricity. The Thorium fuel cycle in a nuclear fuel cycle, is composed of the naturally abundant isotope of Thorium, as the fertile material for nuclear fission. The Thorium in the reactor is transmuted into uranium-233, which is the primary fissile artificial isotope in the nuclear fuel. The main difference between natural thorium and

uranium is that only trace amounts of fissile material such as thorium-231 and uranium-235 are contained in the natural ore materials. These materials are not sufficient to start a nuclear chain reaction (Cox, 1995). Therefore, the natural Thorium must be, additionally enriched, with fissile material and neutron source triggered, for it to sustain a chain reaction (Nema, 2010). In a reactor that contains thorium fuel, Thorium absorbs neutrons in order to produce uranium -233. This reaction matches the process that takes place in breeder reactors which normally use uranium-238. In breeder reactors, fertile Uranium -238 absorbs neutrons to form fissile Plutonium-239. The generated Uranium-233 in a Thorium-fueled reactor can undergo two processes either fissions in situ or undergo chemical separation from the spent nuclear fuel and fabricated into new nuclear fuel. These two processes depend mainly on the design of the reactor and the type of fuel cycle (Heuer, et al. (2014).

1.3 Economic benefits of mining uranium

From the history of civilization and industrial advancement, various minerals have been mined from the earth's crust since pre-historic era for economic development. The continuous evolution and expansion in extraction and utilization of minerals with economic benefits has been made possible through a range of technological innovations. There is even an ancient mining industry axiom which says that *'if you can't grow it, it has to be mined'* (BGS, 2004).

The complex geological setting of Kenya, alongside its coastal continental shelf has contributed much to Kenya's national mineral source wealth (Bubois & Walsh, 2007). The recent discovery of energy rich minerals such as coal and crude petroleum has presented great potential of supporting the development of the *"industrial revolution"* program in Kenya (Bubois & Walsh, 2007). Kenya currently produces a wide range of minerals ranging from gemstones, gold, gypsum, talc, trona and heavy mineral sands. Kenya is also endowed with manganese, zinc, kaolin, pyrite, rare earth elements copper, nickel, chromite, wollastonite, graphite, pyro chlorite, and of course uranium and thorium (Bubois & Walsh, 2007).

Various industries, such as the manufacturing, construction, energy and agriculture require adequate supply of energy for their sustainability. The sources of the renewable energy such as solar and geothermal can be harnessed, and be incorporated in the energy mix to meet part of Kenya's energy requirements. Recycling of the industrial by-products to meet the government environmental and industrial waste disposal requirements, can assist in minimizing the waste products in the ecosystem.

According to the OECD, 2014, the overall global production of uranium increased by 0.2% from 54653 tU in 2010 to 54740 tU in 2011. Noteworthy, production of uranium has experienced a gradual increase in the years, following years up to 2014. Although the rate of increase in production of uranium in Kazakhstan has been reducing in the recent past, the country remains the largest producer of uranium in the world by a large margin. In 2012, uranium production in Kazakhstan totaled more than the combined production in Australia and Canada during the same period. Notably, the second and third largest producers of uranium are Canada and Australia respectively (WNA 2017).

1.4 Occurrence of uranium and thorium minerals

In the year 1789, a German Chemist by the name Martin Heinrich Klaproth, discovered the uranium element. In 1972, Francis Perrin, a Physicist from France, discovered fifteen ancient natural nuclear fission reactors. These natural reactors which are no longer active were located in isolated ore deposits at Oklo mine in the West African Country of Gabon. This remarkable ore deposit has geologically been dated to the Proterozoic era.

Uranium occurs in its natural form as pitchblende and contains three major isotopes; uranium -234 and uranium -238, uranium -235. The natural abundance of uranium is 99.28%, while that of uranium -235 is 0.71% and uranium -234 is 0.0054% (Garnie-Laplace et. al, 2010). All these isotopes are radioactive in nature. However, even though they emit the alpha particles in nature, they all have small probabilities of undergoing spontaneous fission. Uranium also has three other trace isotopes; uranium -239, uranium -237 and uranium -233. The first two isotopes are formed from uranium -238 through neutron capture, while uranium -233 is formed from the decay chain of neptunium-237 (Garnie-Laplace et. al, 2010).

According to Klepper and Wyant (1957) about 103 minerals contain uranium as a constituent element. These are ores which contain more than 1 percent Uranium as an element in each of these minerals. Uranium occurs as tetravalent in about 25 minerals and hexavalent in about 77 minerals. Fifteen of the uranium bearing minerals are either simple or hydrated oxides. About twenty of these minerals are complex titanates and niobates, while fourteen are silicates (Klepper and Wyant, 1957). In addition, seventeen are phosphates, ten carbonates, six sulphates, eight vanadates and eight arsenates. Occurrence of uranium is not only confined to the continental crust, as uranium bearing minerals are also found in marine environments, such as carbonaceous shale (Klepper and Wyant, 1957). Some lignite and coal have also been found, to contain uranium. Uranium can also occur as intergranular films in igneous environments. The principal minerals of uranium in the larger ore deposits are the oxides; uraninite, pitchblende, carbonite and tyuyamunite, and the silicate coffinite, the vanadates, and davidite and the complex titanates brannerite. Uranium is not known in nature as a simple sulfide, arsenide, native element or as a telluride.

In meteorites, Uranium can be found in a few $\mu\text{g/g}$ in both iron and silicate meteorites (Cox, 1995). Uranium can also be found in considerable quantities in rocks such as basic and ultrabasic igneous rocks, intermediate and acidic igneous rocks, and in shale and sandstones (Cox, 1995) on the surface of the earth. Uranium can also be found in sea water, river water, and ground water. In abnormally rich rocks and ore deposits, uranium can be found in fairly large amounts in marine phosphorite, marine and black shale, riebeckite-albite granite, placer deposits, lignite and coal, pegmatite, uraniferous conglomerate, sandstone-type deposits and Nigerian vein deposits, (Tsurikov 2009).

1.5 Radio-ecological hazards associated with mining of uranium and thorium minerals

In general, uranium and thorium mineral mining involves disturbing the environment to a certain degree. Such disturbances may include clearing of vegetation on land, activities related to site development such as removal of overlying material, water consumption and the potential for accidental release of chemicals used in the mining process. In uranium or thorium mines, tailings may contain significant amounts of TENORMS

thereby posing additional dangers associated with radio-ecological hazards. It is therefore as a requirement for a country that plans to undertake to exploit its minerals, to implement a regulatory regime that will regulate the amount and type of discharge to the environment for the protection of people, property and environment.

Various other studies around the world, have revealed presence of high radiation levels, for example, at the coastal region of the Morro Do Forro and Esperito Santo in Minas Gerais situated in Brazil, (Ajlouni et al, 2009); Yangjiang of Guangdong province; southwest coast of India (Sunta, 1993; Selvasekarapandian et al., 1999); Ramsar in Iran (Sorahbi, 1995) and in parts of the Canada and United States (NCRP, 1987). Studies indicate that in Taiwanese houses, the indoor gamma dose rate was found to be higher than in other countries.

In Africa, a few radiometric studies have been done on naturally occurring radioactive minerals (NORMs); Isinkaye et al. (2018) measured radon-226, thorium-232 and potassium-40 in his research on the radiological hazards attributed to the natural radioactivity in Nigeria. Adel, (2004) conducted a research on the radiological effects of NORMs from the sedimentary rocks sampled from the Upper Egypt. Sroor et al (2002) evaluated the dose rate caused by naturally occurring radioactive materials (NORMs) in North Tushki area, southwestern desert of Egypt.

In Kenya, aerial radiometric surveys for uranium prospecting in Kenya have delineated five anomalous radiometric zones; Coastal region, Kerio Valley, Cheptais, south of Lodwar, East of Maralal, North of Eldoret. There are various high background radiation areas in Kenya inclusive of Mrima Hill (Mustapha, 1999; Patel, 1991), Gwasi, Mt. Homa (Otwoma, 2012), Ruri Hills, Homa Bay (Winnam Gulf), Tinderet and Koru. The high background radiation anomaly, in these areas is mostly associated with the sedimentary formations of weathered geological profiles.

Patel has determined that the Mrima area had elevated natural radioactivity levels. His work to study the radiation distribution pattern showed that boreholes in the area contain high radiation anomalies. Mustapha (1999) found elevated levels of ^{226}Ra and ^{232}Th in soils samples from different parts of Kenya; Machakos, Nairobi, Kwale, Trans Nzoia,

Bungoma, Kiambu, and Mombasa districts. Agola (2006) also found high radioactivity in the Olkaria geothermal area waters. Maina et al. (2002) established that the radon-222 levels in 42 mud-constructed houses of Soy region in Kenya's province of Rift Valley.

1.6 The Geology of Cheptais

Cheptais is part of the Western highlands consisting mainly of a peneplain, rising to the east from 1200 to about 1700 meters, underlain by Precambrian rocks invaded by granites and other intrusions. On the south-east, there are plateau highlands (about 2,200 meters above sea level) made up of the Kisii Series of sediments and lavas. Highlands of roughly equivalent altitude forming the Nandi Hills, which are composed of Basement System rocks and granites, separate the lower country of Nyanza from the Uasin Gishu Plateau. Isolated areas within the western belt are mountainous and centers of Tertiary volcanic activity (Mines & Geology Department, 2010).

1.7 Problem statement

The renaissance of uranium exploration efforts can be attributed, largely, to the momentous increase in the price of uranium in the global market from under USD10/lb in the 1990s to about USD50/lb in 2008 (Tsurikov, 2009). Uranium has often been traded as yellow cake (uranium concentrate). The price increase has made the exploitation of low-grade uranium to be more economically viable. The current trend in exploitation of uranium resources in the world have demonstrated that massive uranium reserves can be economically recovered by mining at a relatively low cost (Tsurikov, 2009).

Uranium industry argues that, it has been able to demonstrate that, it can mine its uranium responsibly by employing necessary safety measures and preserving the environment. The current global regulatory regime and safety culture within the uranium industry provides the necessary environment for safe and responsible uranium exploitation. Active actions have been instituted to minimize potential radiation risks.

From the radiometric surveys done, both on airborne and ground follow-up in Kenya, potential areas of uranium and Thorium mineralization have been delineated. Only

limited ground follow-up surveys have been carried out in quantifying data from these areas. Radioelement potential designated studies show high propensity of uranium/thorium mineralization at the Coast, Samburu and Western region, of high prospects of economic radioelement reserves.

The deficit of Kenya's energy requirements for establishment of high load demand industries currently is slowing down industrialization process in achieving its Vision 2030 goals. As a consequence, the Government of Kenya is committed to introducing nuclear power to its energy mix as part of its strategy to mitigate, the increasing demand of power as envisaged in Kenya's Energy and Petroleum Regulatory Authority's (EPRA), Least Cost Power Development Plan (LCPDP).

In principle, two natural actinides are required for economical non-proliferation production of nuclear energy; these are uranium and thorium. Through fission reaction processes, when subjected to sources of low energy neutron flux, energy is released which is transformed to power through energy conversion by thermodynamics (Rankine and Brayton cycles). Potential power output for a commercial generation III & III+ reactors is approximately 1400 MW, currently. However, the sources these actinides materials in our environment as well as their quantification, largely remain unknown in Kenya, to date.

Mineral exploitation is key to Kenya's industrial expansion, specifically by mining of economically viable minerals such as; uranium for possible utilization in nuclear energy industry for electricity production. The Department of Mines and Geology is currently charged with the primary responsibility of exploration of potential mineral resources in Kenya, including uranium and Thorium.

1.8 Objectives of the research

1.8.1 General objective

To evaluate the mineral content and assess the radio-ecological hazards associated with the naturally occurring radionuclides in the soils of Cheptais area.

1.8.2 Specific objectives

- a) To assess the levels of the major constituent elements and activity of naturally occurring radionuclides in the study area;
- b) To delineate and map the background radiation variation in the sampled area;
- c) To determine the extent of radio-ecological hazards in the study area.

1.9 Justification and Scope of the Study

Uranium and thorium can be extracted for export to generate foreign exchange for the country. Kenya can engage in the front end of the open nuclear fuel cycle in exploration, mining and milling. This study complements the other explorations efforts that have been done so far, in which radioactive anomalies have been found during exploratory surveys. This study has analyzed the concentrations of the radioactive elements in Cheptais area as a follow up of the airborne surveys in the past.

Energy is a key enabler for sustainable industrial development in Kenya. Energy minerals such as uranium and thorium can be; mined, milled and fabricated to make fuel for nuclear reactors. Tsurikov (2009) explains that there is resurgence in uranium exploration, which is attributed to a significant increase in the price of uranium on the world market from under USD10/lb of uranium concentrate in the 1990s to around USD50/lb in 2008, thereby making the exploitation of low grade uranium deposits viable.

The department of Mines and Geology has identified a number of anomalies with high propensity of U/Th mineralization at the Coast, Samburu and Western region in Kenya. Further exploration of these anomalies, can be conducted to delineate the spatial distribution and conduct mineral assay and economic viability of these energy minerals for industrial development and economic growth

The scope of this study, was to evaluate the soils for mineral content, and measurement of background radiation levels for radio-ecological hazards determination in Cheptais area. This study is limited to evaluation of the main mineral constituents as well as the naturally occurring radionuclides (^{40}K , ^{238}U and ^{232}Th) activity concentrations in the sub-

soil samples collected from sampled Cheptais area. The study also estimates the radiological hazards from the values obtained from measured ground radiometric survey of the study area. The absorbed dose rate (DR) was determined with the assumption of 1m distance above the ground level. Radium equivalent ($Ra_{(eq)}$), gamma radiation index (I_{yr}), annual effective dose (E), as well as the internal and external hazard indices (H_{in} and H_{ex}) were determined using existing ICRP models.

This study covered an estimated area of 9 km², part of the delineated Cheptais Anomaly area in Bungoma County, during the fieldwork exercise done in December, 2018 in the dry season.

The findings and recommendations of this study, opens up an array of research opportunities that will further enhance the knowledge base of natural resources for future strategic planning on utilization in the country.

CHAPTER 2: LITERATURE REVIEW

2.1 Introduction

Radioactive minerals such as, those that contain uranium and thorium, are critical in the nuclear fuel cycle industry. The Front-end of the nuclear fuel cycle consists of various components namely: fuel fabrication, milling, mining, enrichment and conversion. In Kenya, radioactivity anomalies have been identified at the coast, the rift valley and western regions in airborne surveys.

In this chapter, I have reviewed several studies on naturally occurring radionuclides, specifically on exploration and exploitation of uranium and thorium minerals in general, and in Kenya, and on their radio-ecological hazards in the environment.

2.2 Geology and mineral occurrence in Kenya

In general, the geology of Kenya, shows that, much of the country, is covered by Precambrian Basement, Tertiary volcanics and Quaternary sediments. The geology of Kenya also comprises of coastal terrigenous clastic sediments of the Karroo System belonging to the Jurassic and Tertiary (Lakkundi, 2012). The main geological mineralization sources in Kenya are; the Archean Nyanzian shield in Western parts of Kenya which is characterized by metallic mineralization with potential for iron bearing minerals. On the other hand, the Proterozoic Mozambique Belt which is extensive in Kenyan Central region is characterized by metamorphic minerals such as wollastonite, graphite, corundum, kaolin, kyarite, marble, and gemstones of different varieties are found together with mineral ores that are associated with granitic and basic rocks, such as iron ore and mica (Lakkundi, 2012). Also, the Sedimentary rocks are widespread and it ranges from Paleozoic to recent time which appears to be the possible hosts and sources of gypsum, hydrocarbons, clays, limestone, construction materials and manganese.

Cheptais is an isolated mountainous region in western Kenya's geological setting which is categorized under the tertiary volcanics (Pulfrey & Walsh, 1969). The geology of Cheptais, Cheptais area consists mainly of volcanic rock deposits. These rocks include

agglomerate lavas, tuff and breccia. The main constituents of these volcanic are melane-nephelinite lava which is characterized by boulders that can range in size from small to large sized. The tuffs are also characterized by Silicified fossil wood with calcite cementation. The characteristic cementation appears to be a major enhancer to local weathering of these tuffs. In addition, Cheptais area has phonolitic-nephelinites and minor intrusions of Pre-Miocene Age. A vast section of this area is also highly jointed, a factor which makes it prone to weathering and disintegration, (Mines and Geology, 2010).

Geomorphologically, Cheptais is mainly influenced by the geology of Mt. Elgon region. A cross-section from the western border of Kenya and Uganda towards the South East of the general area shows the tertiary volcanics which are composed of remnants of volcanic depositional environment. This is followed by the Nyanzian which is composed of lavas and pyroclasts. The granites come after the Nyanzian system which is then followed by Tertiary sediments. Figure 2-1 shows the geologic map of Cheptais area.



Legend

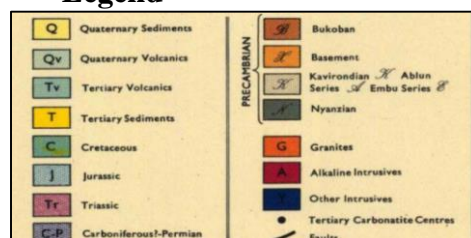


Figure 2- 1: Geological map of Cheptais area

Source: Chief Geologist, Mines and Geology Department (1959).

Kenya's geological setting also contains base metal mineralization, Pb-Zn which is known to be present in the sedimentary basin located at the Coastal belt (Lakkundi, 2012). Heavy mineral sands are also known to be present at the coastal belt.

The volcanic rocks occur at the Rift System in Kenya which yield and host different varieties of construction materials and minerals. These volcanic-sedimentary accumulations have deposits of trona, clays, natural carbon dioxide, diatomite, gypsum and kunkar. Moreover, the geothermal fields are present in this area which has a potential of generating up to 10,000 MWe.

In the southern coastal basin of Mombasa, there is Mrima Hill, a carbonatite ore deposit known to host great amounts some rare earth elements and niobium. This ore has been found to have high amounts of rutile, zircon and ilmenite that contain titanium (Lakkundi, 2012). The main industrial and metallic minerals of Kenya that are economically viable are; talc, iron ore, kaolinite, gold, gemstones, fluorspar, soda ash, heavy sands/REE, coal, limestone and hydrocarbons (Lakkundi, 2012).

The major ore minerals that are either mined or processed in Kenya are; steel, titanium, iron, zircon, aluminum, gold and lead in that order. Both iron and steel industries form approximately 13% of the manufacturing sector thereby contributing greatly to the country's GDP (MoI, 2018). There was a steady increase in production of these minerals between 2011 to 2013. However, except for titanium, the processing and production of these minerals experienced a decline in 2015.

For industrial minerals, Kenya produces soda ash, table salt, fluorspar, lime, sand and industrial glass, carbon dioxide gas, gemstones, cement in that order. The amount of these minerals that have been mined and processed have either stagnated or decreased. This may be attributed to the decrease in the prices of these minerals in the global market or a decline in productivity of the mines (USGS, 2019.). Table 2-1 shows a summary of the main mineral outputs in Kenya.

Table 2- 1: Value of mineral production in Kenya

KENYA: PRODUCTION OF MINERAL COMMODITIES(Metric tons)					
Commodity	2011	2012	2013	2014	2015
Metals					
Aluminum, secondary	14,000	16,000	18,000	17,000	15,000
Gold, mine output, Au	1,636	3,600	2,100	200	300
Iron ore:					
Gross weight	50,000	70,500	--	--	--
Fe content	28,000	40,000	--	--	--
Lead, refined secondary	1,000	1,000	940	1,000	1,100
Titanium:					
Ilmenite concentrate	--	--	5,539	368,239	444,999
Rutile concentrate	--	--	152	59,348	78,947
Zircon	--	--	--	15,004	25,951
Industrial Minerals					
Carbon dioxide gas, natural	15,197	19,919	18,436	19,450	19,750
Cement, hydraulic	4,478	4,694	5,059	5,883	6,353
Clays:					
Bentonite	70	75	80	110	110
Kaolin	1,000	1,000	1,100	1,600	1,600
Other	27,000	28,000	30,000	43,000	43,000
Diatomite	2,039	1,746	1,054	1,195	1,090
Feldspar	35	35	35	40	40
Fluorspar	117,420	110,000	48,500	74,000	63,000
Gemstones, precious and semiprecious:					
Amethyst	16,000	22,100	20,100	8,800	16,000
Aquamarine	290	320	500	220	390
Cordierite, iolite	170	200	300	130	230
Garnet, green	1,205	1,258	1,100	1,210	2,200
Garnet, other	3,600	3,800	15,100	6,600	12,000
Ruby	6,240	6,625	5,500	6,100	11,000
Sapphire	3,500	3,700	3,100	3,400	6,100

Tourmaline	8,800	9,400	34,300	15,000	27,000
Gypsum and anhydrite	6,520	6,653	5,500	5,900	6,400
Lime	52,000	55,000	55,000	57,000	57,000
Salt, refined	253,965	230,872	207,147	223,295	242,100
Sand, industrial; glass	23,000	26,000	21,000	22,000	27,000
Soda ash	499,052	449,269	468,215	409,845	295,417
Vermiculite	515	457	400	440	440

Source: USGS, 2019

2.3 Exploration of Uranium and Thorium in Kenya

In 1952, Sanders made traverses over and around the carbonatite/alkaline intrusive centers of Homa Mountain and Ruri with the purpose of taking soil samples from suitable localities for examination of uranium -bearing minerals. A portable rate meter was used to record radioactivity from rocks and their soil cover recorded in pulses per minute. Both the Homa Mountain and the twin volcanic centers of Ruri, show well defined steeply dipping carbonatite rings which are comparatively resistant to erosion and form conspicuous cliffs and crags. However, the greater part of the hill masses are formed of pyroclastic rocks consisting of calcareous agglomerates and tuffs. Nephelinites and phonolitic nephelinites form a minor part of the volcanic assemblage and occur both as plugs and dykes (Bubois & Walsh, 2007).

Terra Surveys of Canada conducted an airborne spectrometric survey in Coast Province in 1977. The survey covered an area of between 3°15'S to the Southern border with Tanzania and 38°E to the Indian Ocean. The geology of the survey area consists of rocks of the basement system, Coastal Paleozoic sediments, Coastal Mesozoic sediments, intrusions into Coastal sediments, and Coastal sediments of Tertiary and Pleistocene ages. The area east of 39°E (Coastal Belt) got full spectrometric coverage while the area west of this longitude got partial spectrometric coverage. The survey was conducted in an attempt to define regions of any uraniferous mineralization.

In 1978, Macharia and Limion carried out an analysis of the airborne spectrometric survey in the Coastal region of Kenya. In their analysis, all anomalies detected were ranked in

order of priority. Anomalies with uranium counts from 75 cps and above, and U/Th ratios from 1.4 and above were ranked first priority. Those with uranium counts between 50 and 75 cps and U/Th ratios between 1.2 and 1.4 were ranked second etc. First priority anomalies were encountered in Vipingo (2 anomalies), Mombasa (1 anomaly), Vitengeni (2 anomalies), Kinjaro (1 anomaly), and Mwatate (1 anomaly) (Mines and Geology Department, 2010).

In the year 1958, the United Kingdom Atomic Energy Agency carried out an aerial radiometric survey of a probable uranium presence in Kenya and delineated five anomalous radiometric zones. The suspected uranium province consists of the main sediments of Karroo, locally called Duruma sandstones, together with schists and gneisses of the basement system, which form the western boundary, and narrow strip of Jurassic rocks outcrop on the eastern boundary. These are estuarine and marine rocks consisting of mudstones, shale, septarian marl, arkose and sandstone and conglomerate limestone (AEA 1958).

Geosurvey International conducted a regional airborne geophysical survey of the Kerio Valley region and its environs in 1982. The areas were found to be underlain by Precambrian rocks and lie respectively to the west and east of the main East African Rift Valley. The survey isolated a number of prospective areas with good showings for uranium and Thorium (Mines and Geology Department, 2010).

In 1984, a combined team of Kenya and France carried out ground follow-up of the airborne geophysical survey in the Kerio Valley and its surroundings. This was a ground follow-up mineral exploration programme targeting airborne anomalies earlier delineated by Geosurvey International airborne surveys of 1982. The study identified two uranium anomalies at Sigor (Lolmorton anomaly) and Lomut (Rorok Hill anomaly) in West Pokot. The uranium anomaly at Lolmorton occurs as strata-bound roll-front ore body in detrital sediments of the Turkana Grits while the Rorok Hill uranium anomaly is a hydrothermal reconcentration ore body with silicification along north-striking Rift-System faults. The uranium mineralization prospects occur in a north-trending narrow band that extends for more than 20 km. The Rorok survey grid measured over 4.4 km² while the Lolmorton

survey grid measured over 3.5 km². Vertical core drilling was recommended for the Lolmorton prospect since the mineralization is probably concordant while at Rorok, core drilling should be oriented to intercept the mineralization since the mineralization is probably cross-cutting (Mines and Geology Department, 2010).

Additional information obtained from the Ministry of Petroleum and Mining, indicate that uranium and Thorium-232 anomalies have been observed in the following Coastal regions; Vipingo (2 anomalies), Mombasa (1 anomaly), Vitengeni (2 anomalies), Kinjaro (1 anomaly), and Mwatate (1 anomaly). Those in West Pokot include; Two uranium anomalies at Sigor (Lolmorton anomaly) and Lomut (Rorok Hill anomaly). In Barsaloi area in Samburu, the two uranium anomalies are located at the Suiyan River (near the Siambu Complex) and in Raraita area. In Cheptais area; the anomalies are designated as Cheptais, Chesikaki, and Masaba (Mines and Geology Department, 2010). Cheptais and Masaba anomalies are reputed to have high thorium concentrations while Chesikaki has coincident uranium and thorium signatures. Over 440 cps were recorded over Cheptais anomaly while Chesikaki and Masaba recorded over 280 and 220 cps respectively. Very limited ground follow-up surveys have been conducted but these studies have not evaluated the elemental content, mineralogical occurrence and the associated radio ecological impacts of the radioisotopes. Exploratory drilling was recommended for mineral content evaluation (Mines and Geology Department, 2010).

The Mines and Geological Department conducted a ground follow-up survey of three airborne uranium and thorium anomalies in Cheptais that were delineated by Geosurvey International which conducted a survey covering the whole area south of Lodwar, East of Maralal and North of Eldoret.

Mangala, (1987) established the presence of uranium in the Kerio Valley with concentrations of 34 µg/g to 983 µg/g and Mrima hills using EDXRF method. In the study, Thorium and traces of rare earth metals were found in high concentrations (>1000 µg/g). The exploitable amount of uranium in low grade uranium ore is within the concentration range of 100 µg/g to 300 µg/g. He inferred that the presence of uranium in the area was due to the processes of reduction and oxidation given the previous volcanic

activity in the area. He noted that the uranium is not linked to high grade fluorite ore but was transported from the other areas within Kerio Valley (Mangala, 1987).

Patel (1991), in later studies determined that the Mrima area is composed of deeply weathered carbonatite rocks and had elevated natural radioactivity levels. His work to study the radiation distribution pattern showed that boreholes in the area contain high radiation anomalies while the external radiation levels in the Mrima hill ambient atmosphere was found to be fifty-three times higher than the natural background effective dose rate (100 to 200 mrem/year) which is much higher than the global annual effective dose rate. Patel reported that the geological structure of the area is masked by deep soil and weathered rock that cover up to 180 meters in thickness in some places. The residual deposit weathered rocks amount to 7.77×10^6 metric tons (Patel, 1991). Various other studies were conducted in Kenya including Soklo point, Rangwa ring complex, Kuge (Tuige), and Ruri hills in Gwasi, Suba district by McCall, (1958).

2.4 Studies on Radiometric Surveys

Globally, various researches have been conducted over the years in high background radiation areas, though very few studies have been conducted to fully quantify thorium, uranium, and other radioactive minerals in Kenya (Mohammadi et al., 2006).

Investigation of NORM levels in and around high background radiation areas is necessary to among other goals, establish the base-line values for NORM and assess human health and environmental risks associated with the elevated exposure of the radiation. In addition, anthropogenic activities related for instance to quarrying, use and production of phosphate fertilizers, energy production from geothermal and coal, uranium and thorium mining, use of bricks and stones as building blocks and aggregates for construction materials, etc could lead to enhancement of NORM levels and consequently radiation exposure in the environment thereby creating technologically enhanced naturally occurring radioactive minerals (TENORMS). The various exposure and transfer pathways of TENORM in the environment together with the associated radiological impacts on humans have been described by O'Brien and Cooper (1998). Furthermore, an informative view of the typical volumes of NORM waste generated from such

technological processes, the potential environmental and regulatory implications as well as recommendations for NORM waste disposal and remediation of contaminated sites are given elsewhere (Paschoa, 2010; Velzen, 2015).

According to Lin et al (1996), in Taiwanese houses, the indoor gamma dose rate was found to be 72 nSv/h, a level higher than in other countries. The internal radon level, however, was much lower than most indoor radon levels of other countries. In Taiwan, for adults, the annual effective dose was found to be 1.56 mSv comprising 0.58 mSv and 0.28 mSv from land-dwelling external and internal radiations respectively, 0.25 mSv from cosmic rays, and from radon-222 inhalation 0.36 mSv was reported. According to the research, other minor components inclusive of ingestion of radon-222, inhalation of radon-220, cosmogenic radionuclides, were approximated to range in values that are comparable with the global average ranges. In Taiwan, therefore, the natural radiation dose level by year 1995 was reported to be only about two-thirds of the global mean of 2.4 mSv recorded in the UNSCEAR report of 1993 but close to 1.48 mSv which is the Japanese level.

In and around Dhaka city, Bangladesh, Miah et al. (1998) evaluated the radionuclides distribution in soil samples. The activity concentrations of potassium-40, uranium-238, and of thorium-232 and a fission product caesium-137 were assessed by gamma-ray spectrometry and the results compared with the global radioactivity measurements. Concentration values of Cesium-137 found in the samples near the surface ranged from 5 - 10 Bq/kg greater than levels obtained from samples of greater depths. The Potassium-40 concentrations ranged from 402 - 750 Bq/kg with a mean concentration value of 574 Bq/kg, radium-226 (uranium series) ranged from 21 to 43 Bq/kg while range of the concentrations of thorium-228 was between 9-22 Bq/kg. The activity amounts of radium-228 (thorium series) were found to range from 34 - 81 Bq/kg.

In Southern Italy, Bella et al. (1997) conducted gamma ray measurements for thorium-232, potassium-40, and uranium-238 on soils as well as the soils from the island of Ustica where activities reported ranged from 15-164, 16-174 and 201-1,350 Bq/kg respectively. The activity concentrations due to gamma were comparable to the measured and obtained

values from both chemical and mineralogical values analyzed from both XRF and XRD measurements. The reported measured levels of the prehistoric radionuclides matched the magmatological characteristics of the dominant lithology.

Wei, (1980) carried out a study in China to quantify the difference in concentrations of radioactive elements between two areas. The study was done in Yangjiang of Guangdong province known to be high background radiation area (HBRA) in China. The areas neighboring the sampling site was designated as a control area. The background radiation sources were observed to be found near the mountains. The surface rocks were found to be granitic. The study concluded that fine particles of monazite whose origin was the granite rocks in the mountain were washed down by rain for a long period of time. These particles were deposited in the surrounding basin region resulting in the elevation of the levels of the background radiation. The results of the analyzed soil samples indicated that the concentrations from the natural radionuclides in soil were quite different between the two areas. The concentration of thorium-232 was about six times elevated in high background radiation area than in the surrounding area.

Various other studies around the world have revealed presence of high radiation levels at coastal region of the Morro Do Ferro and Esperito Santo in Minas Gerais situated in Brazil, (Ajlouni et al, 2009); southwest coast of India (Sunta, 1993; Selvasekarapandian et al., 1999); Ramsar in Iran (Sorahbi, 1995) and in parts of the Canada and United States (NCRP, 1987).

In Africa, a few radiometric studies have been done on naturally occurring radioactive minerals (NORMs). Isinkaye et al. (2018) measured the average values of radon-226, thorium-232 and potassium-40 in his research on the radiological hazards attributed to the natural radioactivity using HpGe-Detector. The study was done in bituminous soils from tar-sand belt of southwest Nigeria. He found that the levels of these nuclides in the soils were below the global values. Adel, (2004) conducted a research on the radiological effects of NORMs from the sedimentary rocks sampled from the Upper Egypt. He was able to evaluate the average values of Ra representative and equivalent level indices in Egypt particularly, Sarai area. He was able to find the mean absorbed dose rate in the area

to be 141.4 and 136 nGy/h for Sarai and Anz, respectively. From the conclusion, these mean results contributed a mean effective dose of 166.8 and 173.5 $\mu\text{Sv/y}$ respectively. These figures were approximately 16.70 % and 17.40 % of the 1.00 mSv/y accepted by the ICRP, (1993). The soils of the Nile delta were also measured for radioactivity by Ibrahim et al. (1993). From the study, the clay soils recorded highest radionuclide activity while in the sandy soils, lowest concentration activities were observed.

Sroor et al (2002) evaluated the dose rate caused by naturally occurring radioactive materials (NORMs) in North Tushki area, south western desert of Egypt. The activity concentrations due to thorium-232, uranium-238 and potassium-40 were determined to be higher than the international recommended limits as shown earlier in this section. The study indicated averages of 35.75 to 4576.61 Bq/kg for uranium-238, 36.66 to 93,824.18 Bq/kg for thorium-232 and 427.17 to 10,203.18 Bq/kg for potassium-40.

There are various high background radiation areas in Kenya inclusive of Mrima Hill (Mustapha, 1999; Patel, 1991), Gwasi, Mt. Homa (Otwoma, 2012), Ruri Hills, Homa Bay (Winnam Gulf), Tinderet and Koru. The high background radiation anomaly, in these areas is mostly associated with the sedimentary formations of weathered geological profiles, which contain elevated amounts of thorium-232 and uranium-238. Most of the accessible information on this high background radiation area is obtained from the mineral exploration surveys and geological. However, hardly has this high background radiation area anomaly been comprehensively delineated and assessed in the context of its geochemical, spatial, co-dependencies geological and the anthropogenic variability.

Elevated natural radiation exposure levels have also been reported in a number of areas around the world such as Guarapari in Brazil (Cullen and Franca, 1977) and Ramsar in Iran (Sohrabi, 1995). In the case of Ramsar for instance, annual effective doses reported are as high as 132 mGy/y, which is approximately 55 times elevated than the global average. The high background radiation in this case are mainly caused by enhanced ^{226}Ra concentrations and its daughter nuclides in hot springs around Ramsar.

Mustapha (1999) recorded elevated levels of ^{226}Ra and ^{232}Th in soils samples from different parts of Kenya. In a research on the evaluation of exposure of human to natural

radiation in Kenya, geological materials and water samples from distinct geological profiles, specifically the more densely populated areas; Machakos, Nairobi, Kwale, Trans Nzoia, Bungoma, Kiambu, and Mombasa districts were studied. The general average activity concentrations of potassium-40, radon-226 and thorium-232 in the rock samples were evaluated to be 705, 65 and 163 Bq/kg respectively. The approximated effective dose attributed to external exposure due to terrestrial gamma radiation recorded a range of dose rate readings from 0.06 to 2.00 mSv/y with 0.76 mSv/y, being the average dose. Rn concentrations in diverse sources of water were reported to be elevated than the recommended global average of 37.1 Bq/l. As per Maina et al. (2002), a number of samples analyzed reported higher values of thorium-232 and uranium-238 gamma activity levels than the world mean of 40 Bq/kg for the two radionuclides. Agola (2006) also recorded a mean activity level of thorium-232, potassium-40, uranium-238, radium-226 and as 149.33 ± 17.0 , $1,095.20 \pm 53.2$, 73.72 ± 7.4 , 163.81 ± 18.6 Bq/kg respectively in the Olkaria geothermal area. The mean activity concentrations of Rn-222 in water varied from 1.9 ± 0.4 to 8.6 ± 0.1 KBq/m³ with an overall average value of 5.56 ± 0.5 KBq/m³. The Rn-222 values reported from the sources of water (Agola, 2006) were within the accepted concentration of 10 KBq/m³ in water (UNSCEAR, 1993). The average concentration levels for radon-222 in the water of the study area was also far below the US-EPA, (1993) permissible level of 11 KBq/m³ in overall. Rn-222 activity concentration for the indoor environments ranged from 5.13 ± 0.7 to 83.47 ± 0.1 Bqm⁻³ with average figure of 41.05 ± 3.2 Bq/m³ with a value below the recommended levels of 200-600 Bq/m³. Agola, (2006) evaluated annual absorbed dose and effective dose rate in the air as 213.89 nGy/h and 0.53 mSv/y respectively. When compared with the global average figure of 0.46 mSv/y and 57 nGy/h respectively, the area of study, as per Agola (2006), was regarded as high background radiation area. A total mean effective dose due to radon-222 level in water was reported to be 46.55 nSv/y assuming dose to adults only and consumption rate of water as 0.5 liters per day. Effective activity dose rates for indoor radon-222 was observed to be 0.09 mSv/y due to radon gas and 1.87 mSv/y attributed to the short-lived radon daughter nuclides dissolved in soft tissues assuming equilibrium factor of 0.4. The geothermal are was therefore deduced to possess substantial amounts of natural radiation that pose health risks to the residents.

Maina et al. (2002) established that the radon-222 levels in 42 mud-constructed houses of Soy region in Kenya's province of Rift Valley, were all below the 200 Bq m^{-3} which is recommended by UNSCEAR. In Taita and Taveta regions of the country's coastal province, a majority of similar houses surpassed the UNSCEAR limit. Thirteen houses surpassed the recommended limit of 400 Bq m^{-3} , the (UNSCEAR, 1993). Annual effective dose was also computed and ranged from $3.1 - 3.6 \text{ mSv/y}$ in the coastal region and $0.4 - 2.6 \text{ mSv/y}$ in Rift Valley. Based on the African cultural norms, the occupancy factors for the outdoor set at 0.5 and 0.6 for men and women respectively from these regions were used to compute and obtain the effective dose.

CHAPTER 3: METHODOLOGY

3.1 Introduction

This chapter presents a brief description of the study area, materials and sampling procedures used, describes; sample preparation procedures, methods used to determine the elemental content and analytical methods applied in data analyses. In addition, there are sections that, describes the procedures used, for assessments of radiation health hazard risks using the following; absorbed dose rates, annual effective dose equivalent, radium equivalent, external hazard index and internal hazard indices.

3.2 Description of study area

The study area is a localized area in Bungoma County, formerly in Western Province of Kenya. It lies between longitudes $34^{\circ} 27'$ and $34^{\circ}28'$ East and latitudes $0^{\circ} 48'30''$ and $0^{\circ}50''N$. The region borders Kakamega County, Uasin Gishu County, and Uganda and Trans Nzoia County, to the North, the West, the East and the South in that order. The specific area of study is located 450 Km to the North-West of Nairobi, 2 Km due North of Cheptais town and measures approximately 9 Km^2 .

The study area falls within the larger Mt. Elgon region, which according to the 2009 census, has total population of 3,899 and 193 people per square kilometer (CRA, 2013).

The area has a moist to moderately dry climate and receives 3000 mm of rainfall annually with two rainy seasons between April to June and September to November. The temperature of the region ranges between $15.9^{\circ}C$ to $30.5^{\circ}C$. The region is a major water catchment area, whose vegetation is typical of mountainous regions, includes a series of vegetation zones ranging from montane forest zone, bamboo and low-canopied forest and high montane health zone. Figure 3.1 shows the meteorological data of study area, for the period between 1993-2013 (Bomuhangi et al, 2016).

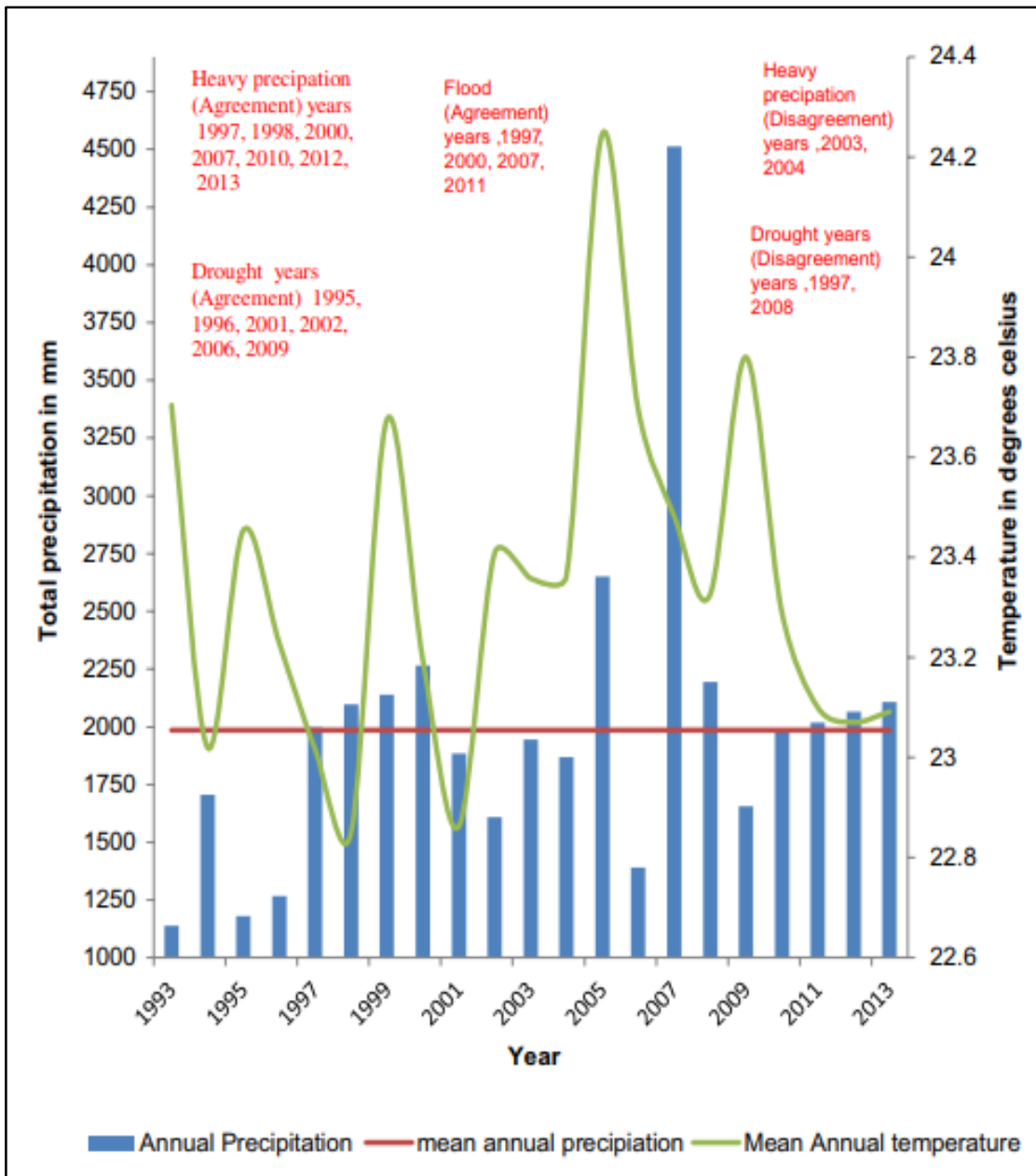


Figure 3- 1: Meteorological data of Cheptais area

(Source: Bomuhangi et al, 2016)

The main cash crops grown in the area, include; coffee and tea which are planted in small scale farms. Other cash crops include; bulbous onions and tomatoes. Maize is a subsistence crop which is planted in small scale farms alongside other crops such as beans, sweet potatoes and cassava. In addition, arrowroots are planted along river courses. The people of Cheptais also keep livestock.

3.3 Field Sampling and Measurement

3.3.1 Radiometric Survey Measurements

The radiometric survey was done using an ionizing radiation measuring meter, RSKB-104 to measure gamma radiation field equivalent dose rate in the sampled areas. This is a Geiger counter, which is an individual dosimeter and radiometer designed for radiation monitoring of terrain, living accommodations and industrial premises. It is used to measure gamma radiation field equivalent dose rate, and specific radioactivity of cesiums-137. Five readings were recorded for each site and these readings were used to obtain the mean values.

A heat map was generated from the radiometric survey measurements using ArcGIS 10.6 software. Kernel density analysis was used to define the population parameters of each grid cell whereby the sampling site was set as the central position of the grid and a number of arbitrary GPS coordinate values added to the grid depending on the dose rate measurements. This is because for Kernel density tool to execute effectively, the dose rate readings have to be converted to a form of spatial distribution. To do this, the survey meter readings were converted to spatial data by addition of a number of arbitrary GPS coordinates proportional with the dose rate readings within the grid cell of the sampling sites. The obtained field measurement values were categorized into four (4) classes with distinct colors each representing a range of levels of dose rates measured in the field. These classes were categorized as follows; green (between 0 - 0.15 μSv), jade (0.16 - 0.30 μSv), amber (0.31 - 0.45 μSv) and red (0.46 - 0.60 μSv). The lowest class (green) had only one GPS coordinate hence there was no additional point to be added on the specific grid cells that had values of less than 0.15 μSv . One additional coordinate was added to each grid cell that had values ranging between 0.16-0.30 μSv , two coordinates were added to each grid cell that had sampling points measured readings of between 0.31-0.45 μSv while three additional points were added to grid cells with values higher than 0.45 μSv .

3.3.2 Soil Sampling for Mineral Content Analysis and Radioactivity Measurement

Sampling of the soils involved the following; a grid sampling method was used, whereby a square grid of equally spaced lines was established. Each line was spaced at a distance of 0.5 km to form square grid cells. The center of each grid cell was then identified. From this center, an area 10 m radius was established within which one soil sample from the center of the circle was collected. The top humus soil was removed in order to collect only the subsoil. The subsoil samples were collected from the central point of each grid cell at depth between 20- 30 cm. All the soil samples from each grid cells were labeled as G1, G2, G3, to G36 in sealed sampling cans weighing about 500 g then transported to the laboratory for analysis.

A total of 36 representative soil samples of the study area were collected using an auger, during the fieldwork exercise done in December, 2018 – in a dry season.

Rock outcrops in the area were also sampled and one fresh rock sample was collected from each rock outcrop. A geological hammer was used to collect the rock samples, packaged and shipped to the laboratory for further preparation and analysis. A total of seven (7) rock outcrops were sampled. Figure 3- 2 shows the map of the sampled sites within Cheptais area.

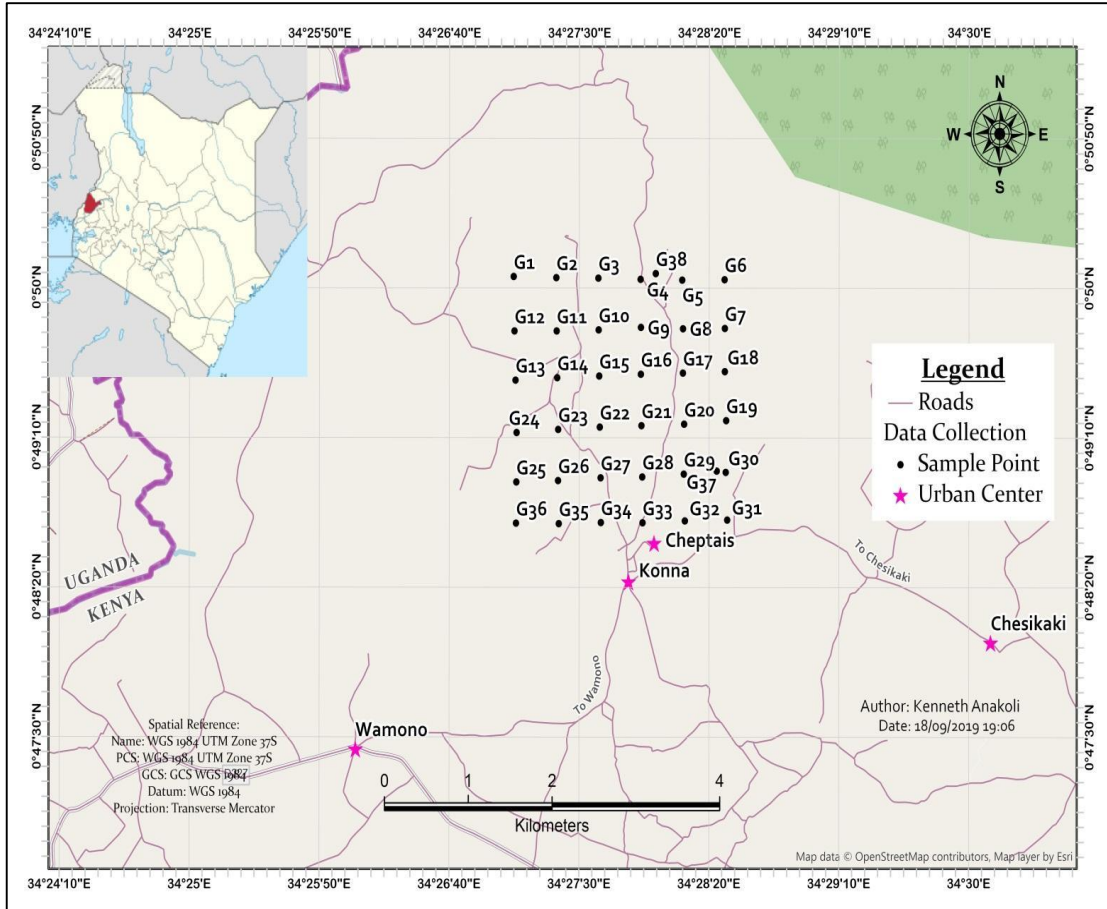


Figure 3- 2: Map of the sampled sites within Cheptais area

3.4 Sample preparation for EDXRF analyses

The rock and soil aggregate sampled from the study area were initially air dried for two weeks and then oven dried to a constant weight, thereafter. The soil samples were then crashed using electronic pestle and mortar followed by sieving using a 75µm sieve to remove any organic debris, such as leaves, stones, and twigs before storing them in the plastic containers for further preparations. Both the soils and the rock samples which were collected were prepared in a similar way.

For EDXRF analysis, the samples were further pulverized in mortar and pestle sieve through a 60-100 µm sieve. Portions of the sieved samples were then diluted with starch binder in the ratio of 1:4 and homogenized by mixing thoroughly. Three pellets of

sample aliquots each weighing about 300 mg were prepared using a hydraulic press for elemental content analysis.

3.5 Sample Preparation for Radiometric Analysis

For radioactivity analyses, pulverized samples were each weighed to approximately 300-400 g and sealed in 200cc plastic containers. Samples were left to settle for two (2) months to remove gaseous radon which has a half-life of 3.8 days, and ^{214}Bi and ^{214}Pb known to be its short-lived decay daughters to reach natural stability with the long lived ^{226}Ra isotope. The background radiation was estimated from measurements of the empty containers before the analysis of the samples. Basically, each sample was transferred into a sample holder in a shielded HpGe detector container and measured for 12 hours. Lead-212 and lead-214 photo peaks at 238 keV and 609 keV were used to identify thorium-232 and uranium-238, respectively.

3.6 Determination of Elemental Content and Radioactivity Concentrations

3.6.1 EDXRF Technique for Elemental Content Analysis

The EDXRF spectrometer that was used in this study, is an AMPTEK X-123 Energy Dispersive X-ray fluorescence spectrometer, which consists of an X-ray generator as the excitation source operated at 5-50kV. The tube current is varied between 1-1000 μA . The primary X-ray filters can be switched between five types with an exposure area of 10mm in diameter for manual settings while the automatic setting has 1, 3, 5- and 10-mm diameter available. The instrument also includes a semiconductor Si (Li) detector 10 mm² mounted at 45° take off angle with respect to the sample. The instrument has a large sample chamber which can open and close automatically. The chamber has a width of 300 mm and 150 mm height. The data processing unit consists of a Personal Computer with a hard disk drive, a Windows 7 operating system and pre-installed factory produced software for both qualitative and quantitative measurements.

The element' Lower limits of detection (LLD) were evaluated by using equation 3.1.

$$LLD = 3 \frac{C\sqrt{R_b}}{P} \quad (3.1)$$

Where: R_b is the background area of the element of interest

P is the peak area of the element of interest

C is the concentration of the element of interest in $\mu\text{g/g}$.

The EDXRF operating principles schematic diagram is shown in Figure 3-3.

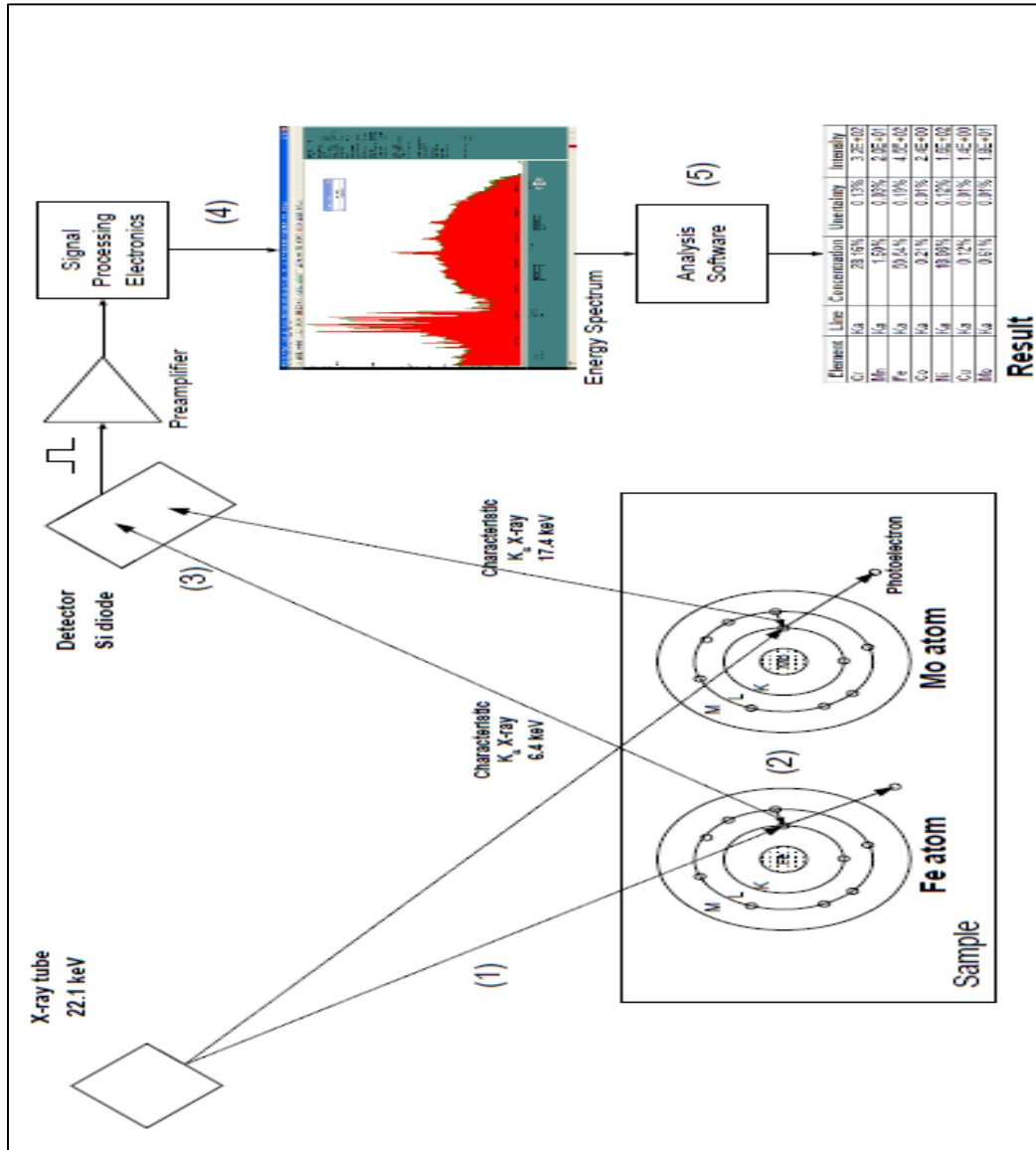


Figure 3- 3: Schematic diagram of the operating principle of EDXRF

Each sample pellet was irradiated for 200 seconds live time after which quantification and qualitative analysis of the X-ray spectra was done by utilization of the AXIL- QXAS software. The spectral data obtained had an energy resolution of 140 eV for (Mn-K α)

X-rays at 5.9 KeV. Figure 3-4 shows a typical EDXRF instrument available at the Institute of Nuclear Science & Technology in the University of Nairobi.

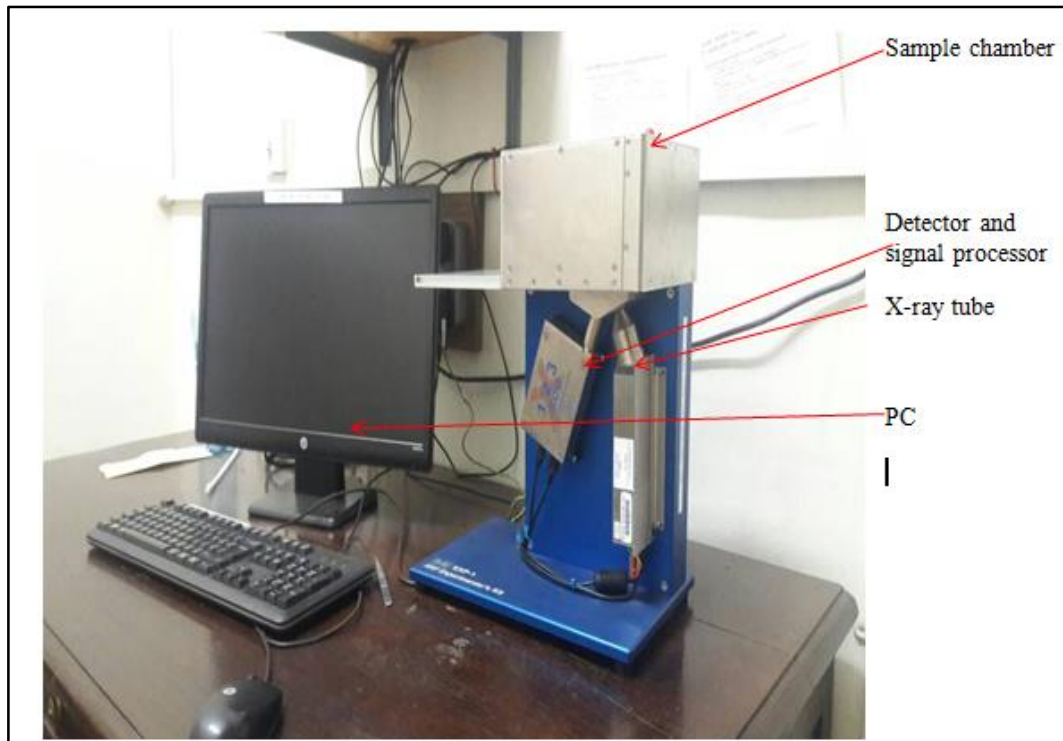


Figure 3- 4: EDXRF instrument at the INST, University of Nairobi.

3.6.2 HpGe Gamma Spectroscopy for Radioactivity Measurements

The gamma spectrometer used is a coaxial HpGe detector available at the Institute of Nuclear Science & Technology laboratories at the University of Nairobi. The efficiency of the detector is 30% relative to the NaI (Tl) detector. The HpGe Detector is considered as one of the best detection instrumentations based on its high sensitivity and efficiency (Knoll, 2000). The detector is designed to detect, measure, process and analyze the activity of gamma emitting radioactive radionuclides. The detection unit consists of the coaxial or planar HpGe detector with an energy resolution of 0.9 at 1332.5keV. The instrument is housed in a lead shield protective chamber connected to a data processing unit, which consists of a Personal Computer with a hard disk drive, a Windows 7 operating system and pre-installed software for both qualitative and quantitative measurements.

Figure 3-5 shows the HpGe instrument present at INST, University of Nairobi.

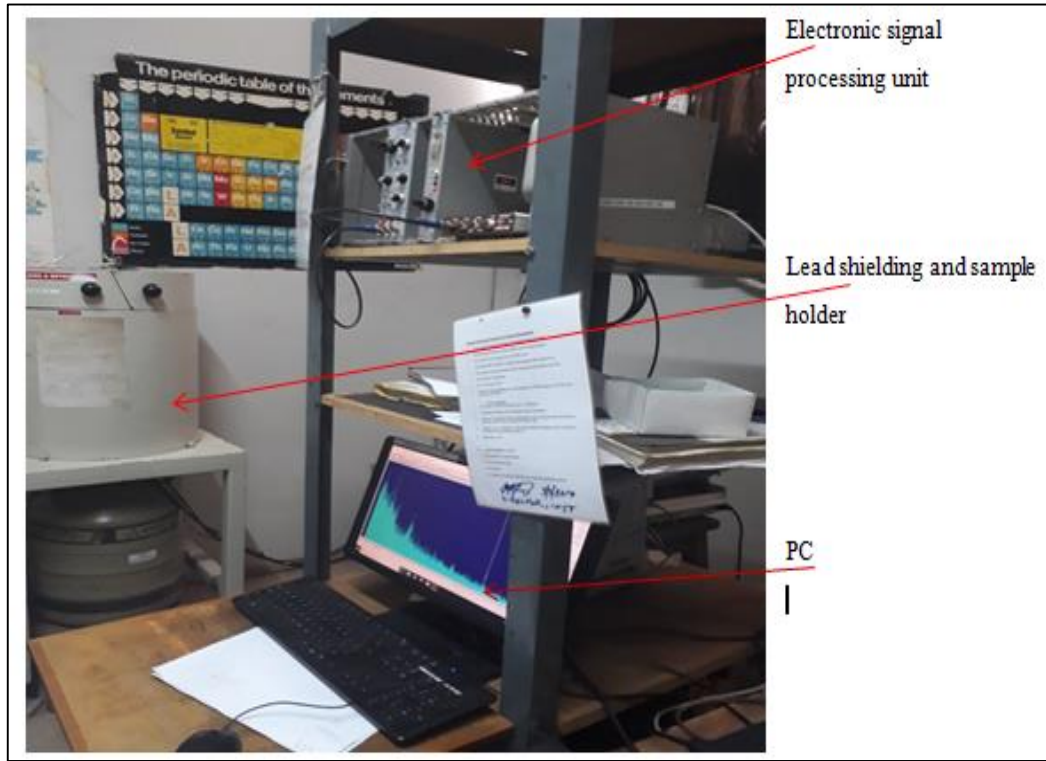


Figure 3- 5: HpGe instrument at INST, University of Nairobi.

For activity concentration measurements, this study used three standard references as a comparative method to determine the corresponding activities. These are; IAEA-RGK-1, IAEA-RGU-1 and IAEA-RGTh-1. This method involves direct comparison of the intensities of the radionuclides in the reference standard to that of the sample. The idea is to effectively reduce matrix effects such as self-attenuation and coincidence summation and half-life correction will subsequently be terminated. The effects due to density are minimized by adoption of similar geometry as that used to measure both reference material and the sample. The results were used to determine the various radiation hazard indices.

Table 3-1 shows the results of certified activity concentrations for the three radionuclides determined using High Purity Germanium detector. This is from an

inorganic/ore material that was available at the Institute of Nuclear Science & Technology from 30th December 1991. These values were corrected for the decays.

Table 3- 1: IAEA-RGK-1: Certified reference material activity concentration, (Bqkg-1)

Radionuclide	Certified Activity conc.	Certified range
²³² Th	3250	3160-3340
²³⁸ U	4940	4910-4970
⁴⁰ K	14,000	13600-14400

The activity concentration levels of ⁴⁰K, ²³²Th, and ²³⁸U in the representative samples were determined based on the photo peaks of the emitted gamma-rays. The ²³²Th activity amounts was evaluated from the intensities of the daughter nuclides, ²²⁸Ac and ²¹²Pb in the collected samples, while that of ²³⁸U equivalent was computed from the mean activity levels of the daughter nuclides ²¹⁴Bi and ²¹⁴Pb of uranium-238 decay series respectively (Gilmore & Hemingway, 1995).

In practice, different radionuclide concentrations depend on the sampled soil types. The soils of Cheptais region were sampled to determine their radiation hazard indices. This was determined from their respective gamma activities of NORMS of interest. In this study, the 1460.8keV gamma line was used for potassium-40. Determination of the thorium-232 was done by calculating the mean activity of actinium-228 and lead-212 which have corresponding energies of 911.1 keV and 238.63 keV respectively. Also, determination of uranium -238 was done by calculating mean activity of lead-212 and bismuth-214 which have corresponding energies of 351 keV and 609 keV respectively

In this particular study, the standard reference materials from the IAEA; RG-K, RG-Th, Soil-375 and RG-U were used.

The levels of radioactivity of ²³²Th, ²³⁸U and ⁴⁰K were determined using equation 3.2 (Gilmore & Hemingway, 1995).

$$\frac{A_s M_s}{I_s} = \frac{A_r M_r}{I_r} \quad (3.2)$$

Where:

M_s is the mass of the sample being analyzed,

M_r is the mass of the reference material

I_s is the intensity of the activity in the sample

I_r is the intensity of the activity of the reference material

A_s is the sample activity

A_r is the activity levels of the reference material

The Oxford PCA3 v.1 software was used to perform simultaneous fitting and identification of all the significant photo-peaks in the spectra. The software displays menu driven reports that included centroid channel energy, FWHM of identified peak, net peak area, background counts, intensity and percentage margin of uncertainty. Table 3.2 provides the energies of the NORMS of interest in the samples, used in this study.

Table 3- 2: Recommended energy lines for gamma-ray emitters of environmental samples

Radionuclide	Isotope(s)	Spectral line (KeV)
K- 40	^{40}K	1460.81
Th- 232	^{212}Pb ^{228}Ac	238.63 911.21
U-238 (^{226}Ra)	^{214}Pb ^{214}Bi	351.92 609.31

The detection limits (DL) for the radionuclides was determined using equation 3.3.

$$DL = \frac{3C\sqrt{B_g}}{PA} \quad (3.3)$$

Where: B_g is the background counts obtained from a gamma peak

PA is the net area under respective gamma photo peaks

C is the levels of activity of the specific radionuclide measured in Bq/Kg.

3.7 Determination of Radiological Radiation Hazard Indices

Radiological data analysis was performed on the results of soil radioactivity measurements to determine the various radiation hazard indices. This was done using existing models and the results compared with those of UNSCEAR permissible limits.

3.7.1 Radium Equivalent Activity, gamma index, external and internal hazard indexes

In the calculation of Radium dose equivalent calculations, the weighted mean activity concentrations of lead-212 and bismuth-214 were used. To assess the radiological hazards, the activity caused by radium equivalent (Ra_{eq}) was used due to gamma ray radiation. Radiological hazards due to gamma radiation were computed for gamma index (I_{yr}), external hazard index (H_{eq}) and Internal hazard index (H_{in}). These indexes were obtained from calculations of values that were acquired from the radioactivity measurements of NORMS using equations 3.4, 3.5, 3.6 and 3.7 respectively (Sowmya et. al, 2010)

$$Ra_{eq} = 1.43 A_{Th} + A_U + 0.077 A_K \quad (\text{Eq. 3.4})$$

$$I_{yr} = \frac{1}{150} A_U + \frac{1}{100} A_{Th} + \frac{1}{1500} A_K \quad (\text{Eq. 3.5})$$

$$H_{ex} = \frac{A_U}{370} + \frac{A_{Th}}{259} + \frac{A_K}{4810} \quad (\text{Eq. 3.6})$$

$$H_{in} = \frac{A_U}{185} + \frac{A_{Th}}{259} + \frac{A_K}{4810} \quad (\text{Eq. 3.7})$$

Where: A_U - Specific activities of ^{238}U

A_{Th} - Specific activities of, ^{232}Th

A_K - Specific activities of ^{40}K

Where the unit of measurement is in Bq kg-1

3.7.2 Absorbed dose

Another way to determine these radiation hazard indices in the environment is through absorbed dose rate in air. This is calculated taking into account a distance of 1m above the ground and the obtained output of the activity concentration levels of the NORMs; ^{40}K , ^{232}Th and ^{238}U , using equation 3.8(Samreh et al 2014) as shown below.

$$D = 0.427A_U + 0.662A_{Th} + 0.043A_K \quad (\text{Eq 3.8})$$

Where: A_U , A_{Th} and A_K are Activities of uranium-238, thorium 232 and potassium-40 respectively

3.7.3 Annual Effective Dose

The annual effective dose equivalent (E) which is received by individuals in Cheptais area was calculated using equation 3.9 (Samreh et al 2014). These values were obtained from the evaluated absorbed dose (D). There is also a dose conversion coefficient (Q) of 0.7 Sv Gy^{-1} , which is the value recommended by the UNSCEAR for adults, was used to convert the ambient absorbed dose rate in air to the effective dose, and the outdoor occupancy factor (f) of 0.4 (Mustapha et al. 1999).

$$E = TfQD \quad (\text{Eq 3.8})$$

Where; T = total seconds per year.

3.8 Statistical Data Analysis

The regression model that was used to estimate the relationship between two variables is a Microsoft excel model. Regression analysis summarized the quantity of change in one variable that is associated with change in the second variable. This regression model assigned one of the variables the position of an independent variable, and the other variable as dependent. The independent variable was regarded as causing changes in the dependent variable. The model does not provide certainty of causal relationship. However, when one variable is fixed as independent variable, then the way in which this

independent variable associates with variations in the dependent variable could be assessed. In order to use the regression model, the expression for a straight line was examined first.

The dependent variable is assigned a Y variable while the independent variable is labeled as the X variable. The aim of the regression model is to determine a linear relationship between the variances. The straight line joining any two points of the X and the Y vales can be stated algebraically as $Y = a + bX$ where; a is the Y intercept and b is the gradient of the line.

The correlation coefficient is represented by the “r” value; where for example, r is greater than $r = + 0.50$, is a strong positive correlation between the two variables. On the other hand, when r is less than $- 0.50$, then there is a strong negative correlation between the two variables. On the other hand, a correlation coefficient closer to $r=0.00$ means there is no relationship between the two variables. However, the most important r values for a meaningful relationship are those with a correlation coefficient with values of $+0.30 < r < -0.30$.

CHAPTER FOUR: RESULTS AND DISCUSSIONS

4.1 Introduction

In this chapter, the results of radiometric survey measurements and those of elemental and activity measurements of soil and rock samples are presented and discussed, using both tables and a heat map of background radiation levels of the study area. I have used graphs to show linear interdependence between variables; trends with histograms, and for variations, using figures and pie charts. I have also provided evidence of validation of the analytical methods

The radiation hazards indices have been determined using results of radiometric measurements for uranium-238, potassium-40 and thorium-232 and the relevant models.

In summary, these results indicate a significant variation in background radiation in the study area. The activity concentration of ^{238}U , ^{40}K , and ^{232}Th and Ra_{eq} , radium equivalent, all exceed the global limits, except for the absorbed dose rates. Iron and potassium were identified as the two major constituents in the soil and rock samples.

4.2 Quality Assurance of EDXRF Analytical Results

To validate the analytical procedure used by EDXRF of the study, a standard reference material, IAEA-PTXRF-09, was analyzed. The reference material is a clay sediment sample containing a wide range of elements and similar matrix as the analyzed samples. The elements of interest ranged from potassium ($Z = 20$) to uranium-238 ($Z = 92$). The elements were present at varying concentrations ranging from trace to major constituents. The results of experimental measurements were compared with the certified values and tabulated in Table 4-1, which shows the experimental values, certified values and certified range of some of the standard reference materials developed by the IAEA.

In general, the obtained experimental values were comparable to the certified recorded values in this study. The results of elemental analysis can be shown using a soil spectrum

obtained from EDXRF analysis. This spectrum displays the intensity of the counts on y-axis as counts rate, while the x-axis is represented by the energy in keV.

Table 4- 1: Results of Analyses of Standard Reference Material, IAEA-PTXRF-09

Element	Experimental value (BqKg⁻¹)	Certified value (BqKg⁻¹)	Certified range (BqKg⁻¹)	Ref. std deviation (%)
K	18.3 ± 1.1	19.9 ± 0.32	19.6 – 20.2	8.0%
Fe	28.6 ± 1.6	29.8 ± 0.95	28.9 – 30.8	4.0%
Cu	19.7 ± 3.0	22.0 ± 0.17	21.8 – 22.2	10.5%
Mn	1.0 ± 0.1	0.94 ± 0.03	0.9 – 1.0	6.4%
Zn	101.7 ± 4.2	102.5 ± 3.9	98.6 – 106.4	0.8%
Th	9.1 ± 0.5	10.8 ± 0.5	10.3 – 11.3	15.7%
U	2.8 ± 0.2	3.1 ± 0.1	3.0 – 3.2	9.7%
Pb	43.1 ± 8.2	37.2 ± 3.1	34.1 – 40.3	15.8%

4.3 Results of Field Measurement: Background radiation levels in the study area

Table 4-2 and Figure 4-1 show the recorded values of field measurements by a hand held survey meter with the corresponding coordinates of the sampling area and the distribution of the dose rates in the sampled sites respectively. The background radiation dose rates of the study area ranged from 0.13±0.06 µSv at site G36 to 0.53±0.08 at site G16, with mean value of 0.22±0.05 µSv. Generally, these results indicate a significant variation in background radioactivity suggesting that the naturally occurring radionuclides are randomly distributed throughout the study area. Patel (1991), when he was conducting a survey on environment hazards of natural radioactivity levels of Mrima hills in Kenya, observed great variability in external dose values ranging from

100 to 200 mrem/year. These results range are within the average global background radiation levels of 0.25 $\mu\text{Sv/h}$ (WNA, 2017).

Table 4- 2: Survey meter measurements, n=5, $\mu\pm 1\text{SD}$

Sample Code	Northings	Eastings	Survey Meter Reading ($\times 10^{-2}$) $\mu\text{Sv/h}$
G1	0°50'3.84"N	34°27'4.75"E	22.8 \pm 2.6
G2	0°50'3.47"N	34°27'21.14"E	14.6 \pm 2.3
G3	0°50'3.32"N	34°27'37.34"E	16.4 \pm 3.9
G4	0°50'2.94"N	34°27'53.59"E	18.2 \pm 3.1
G5	0°50'2.70"N	34°28'9.60"E	20.2 \pm 3.9
G6	0°50'2.84"N	34°28'25.92"E	16.6 \pm 3.4
G7	0°49'46.56"N	34°28'26.03"E	18 \pm 6.3
G8	0°49'46.44"N	34°28'9.92"E	17.6 \pm 3.4
G9	0°49'46.89"N	34°27'53.74"E	16.4 \pm 6.3
G10	0°49'46.04"N	34°27'37.46"E	36.8 \pm 6.0
G11	0°49'45.66"N	34°27'21.30"E	17.4 \pm 3.8
G12	0°49'45.65"N	34°27'5.07"E	19.5 \pm 4.7
G13	0°49'29.22"N	34°27'5.48"E	19.7 \pm 3.8
G14	0°49'30.04"N	34°27'21.54"E	20 \pm 4.6
G15	0°49'30.62"N	34°27'37.69"E	24.5 \pm 7.0
G16	0°49'31.23"N	34°27'53.72"E	53.2 \pm 8.4
G17	0°49'31.63"N	34°28'9.90"E	18.6 \pm 5.6
G18	0°49'32.12"N	34°28'26.04"E	18.2 \pm 7.8
G19	0°49'15.75"N	34°28'26.56"E	20.7 \pm 4.9
G20	0°49'14.57"N	34°28'10.39"E	38.6 \pm 4.8
G21	0°49'14.05"N	34°27'53.96"E	24.4 \pm 5.9
G22	0°49'13.56"N	34°27'37.92"E	18.6 \pm 4.7
G23	0°49'12.76"N	34°27'21.92"E	19.8 \pm 5.3
G24	0°49'11.72"N	34°27'5.91"E	16.0 \pm 4.0

Sample Code	Northings	Eastings	Survey Meter Reading ($\times 10^{-2}$) $\mu\text{Sv/h}$
G25	0°48'55.20"N	34°27'5.82"E	19.8 \pm 4.9
G26	0°48'55.67"N	34°27'21.88"E	15.8 \pm 0.4
G27	0°48'56.61"N	34°27'38.26"E	21.6 \pm 2.1
G28	0°48'56.91"N	34°27'54.28"E	23.8 \pm 1.9
G29	0°48'57.88"N	34°28'10.27"E	26.6 \pm 7.2
G30	0°48'58.47"N	34°28'26.42"E	26.2 \pm 6.3
G31	0°48'42.55"N	34°28'27.00"E	21.4 \pm 4.5
G32	0°48'42.25"N	34°28'10.69"E	27.0 \pm 4.8
G33	0°48'41.60"N	34°27'54.42"E	25.4 \pm 5.8
G34	0°48'41.67"N	34°27'38.36"E	17.5 \pm 3.1
G35	0°48'41.29"N	34°27'22.18"E	17.3 \pm 1.5
G36	0°48'41.45"N	34°27'5.71"E	13.2 \pm 5.6
Mean			22.1\pm4.5
Minimum			13.2\pm5.6
Maximum			53.2\pm8.4
SD			4.5

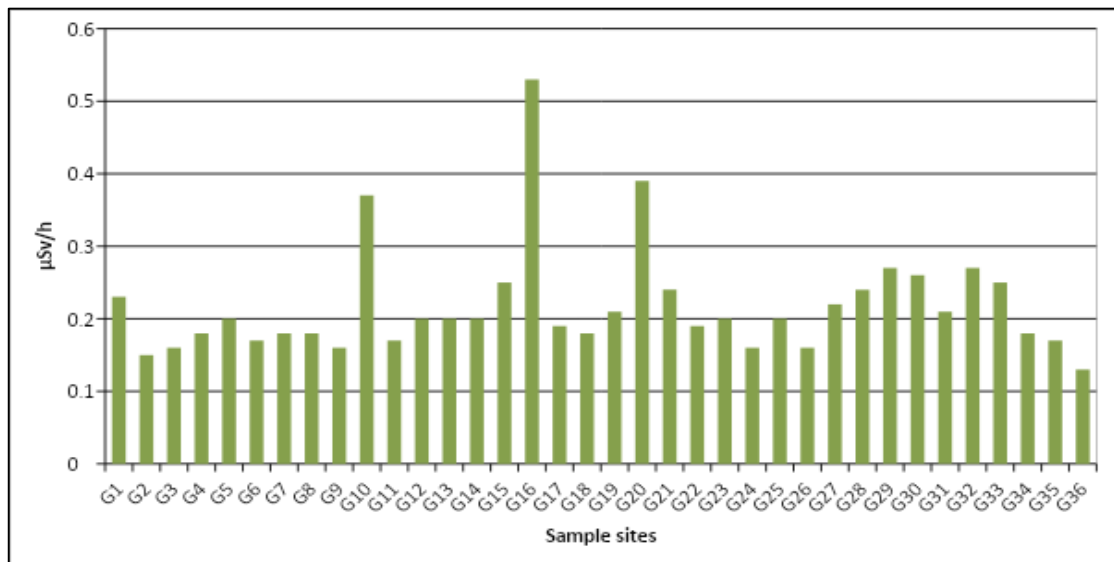


Figure 4- 1: Distribution of background radiation in the sampled sites

Figure 4-2 is the heat map of the study area north of Cheptais town shows the variation of background radiation levels. The results indicate that the study area, is certainly not a high background radiation area, except for the approximately 15% of the area, that has high dose rates. Therefore, most of the study area, does not fall within the target area, earlier identified during the aerial radiometric surveys and hence there was an offset towards the western regions of the target area.

The area with the highest background radiation readings suggest that a number of localized active geological phenomena may be contributing factors; soil erosion and gradual exposure of these radionuclides or deposition and local concentration of the naturally occurring radionuclides, amongst others. Leaching of these radionuclides due to occurrence of a buried ore containing these radionuclides cannot be completely ruled out at this stage.

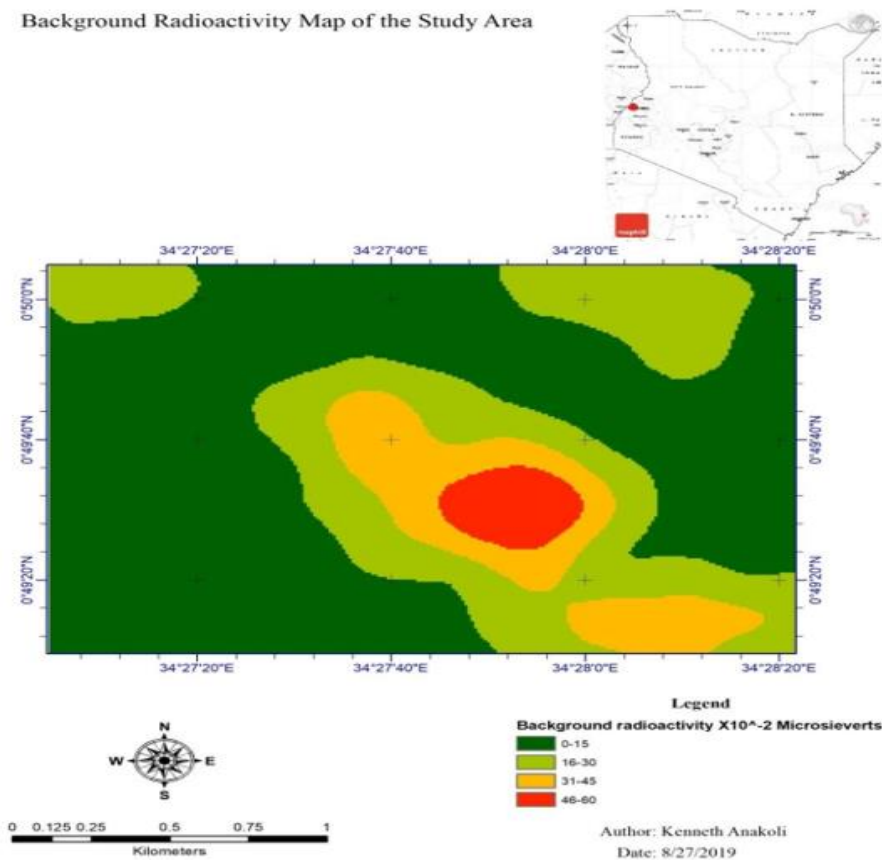


Figure 4- 2: Heat map of the study area showing the variation of background radiation levels

4.4 Elemental Distribution in Soils

Figures 4-3 to 4-10 show the graphs of variations of the concentration of elements Cu, Fe, Mn, Zn, Pb, Th, U and K in $\mu\text{g/g}$ using the tabulated values in Appendix I.

From the results of elemental analysis, iron and potassium were the two major constituents. Other constituents were; manganese, copper, zinc, lead, thorium-232 and uranium-238, which are present only as trace elements. The results indicate that these elements are present in the soils as follows; K (236-37166) $\mu\text{g/g}$, Mn (89-22933) $\mu\text{g/g}$, Fe (1972-289800) $\mu\text{g/g}$, Cu (104-817) $\mu\text{g/g}$, Zn (29.0-672) $\mu\text{g/g}$, Pb (17.0-74.6) $\mu\text{g/g}$, Th (0.9-209) $\mu\text{g/g}$ and U (7.3-20.2) $\mu\text{g/g}$.

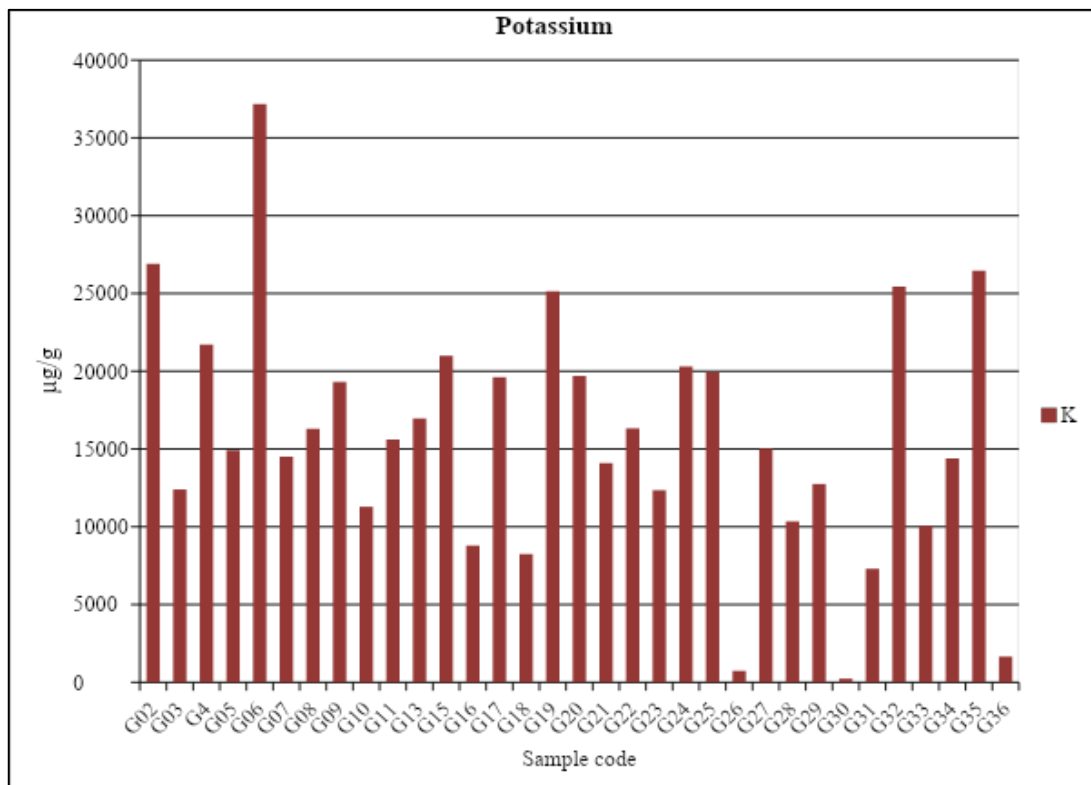


Figure 4- 3: Variation of concentrations of potassium-40

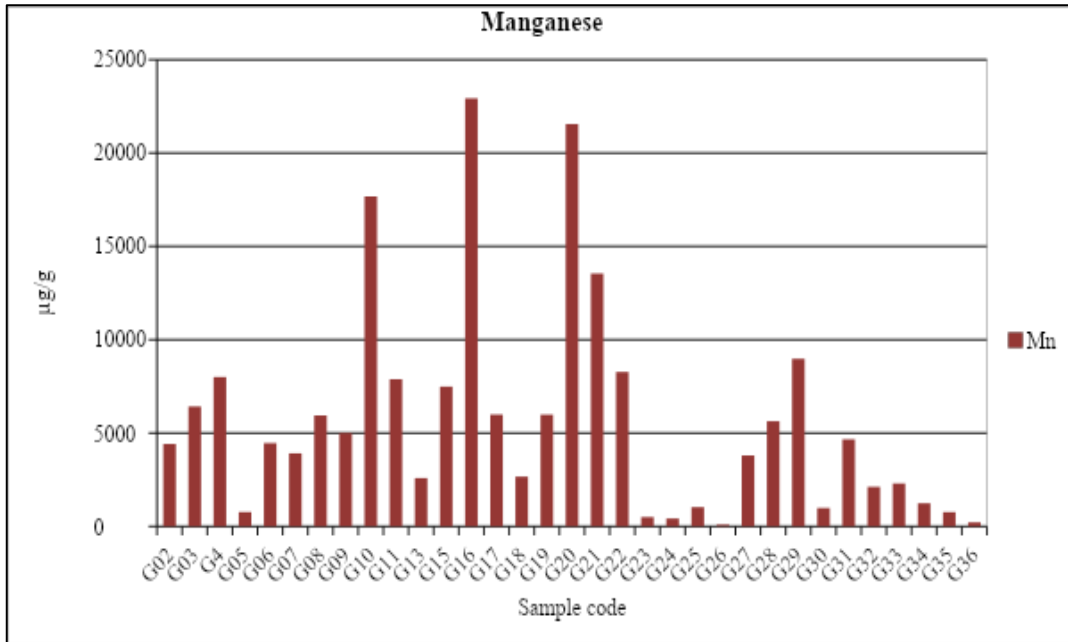


Figure 4- 4: Variation of concentrations of Manganese

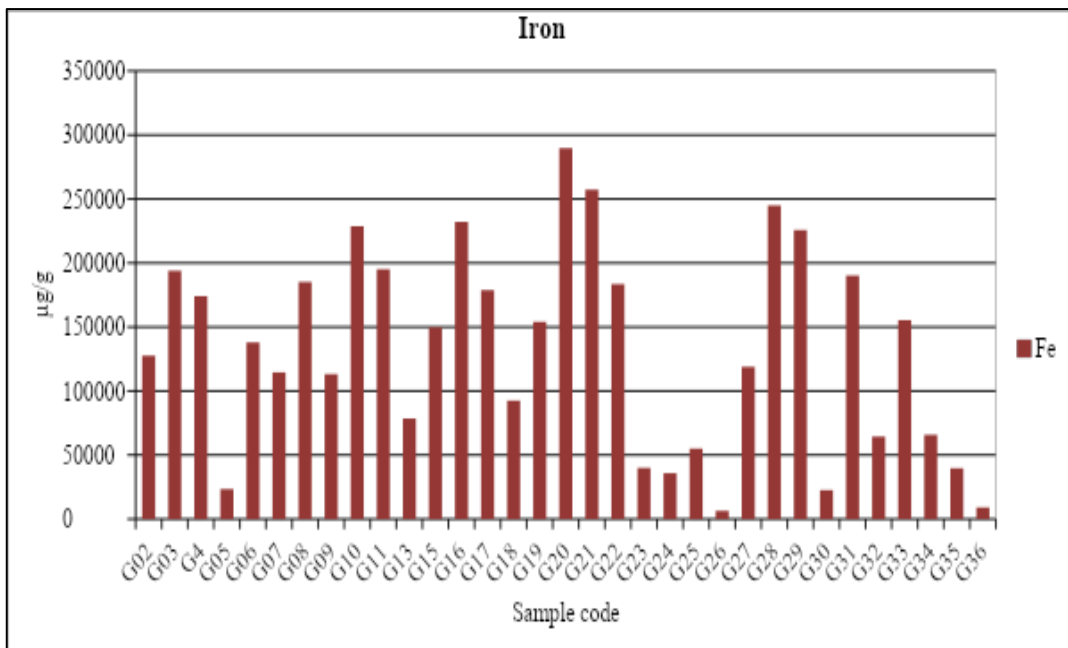


Figure 4- 5: Variation of concentrations of iron

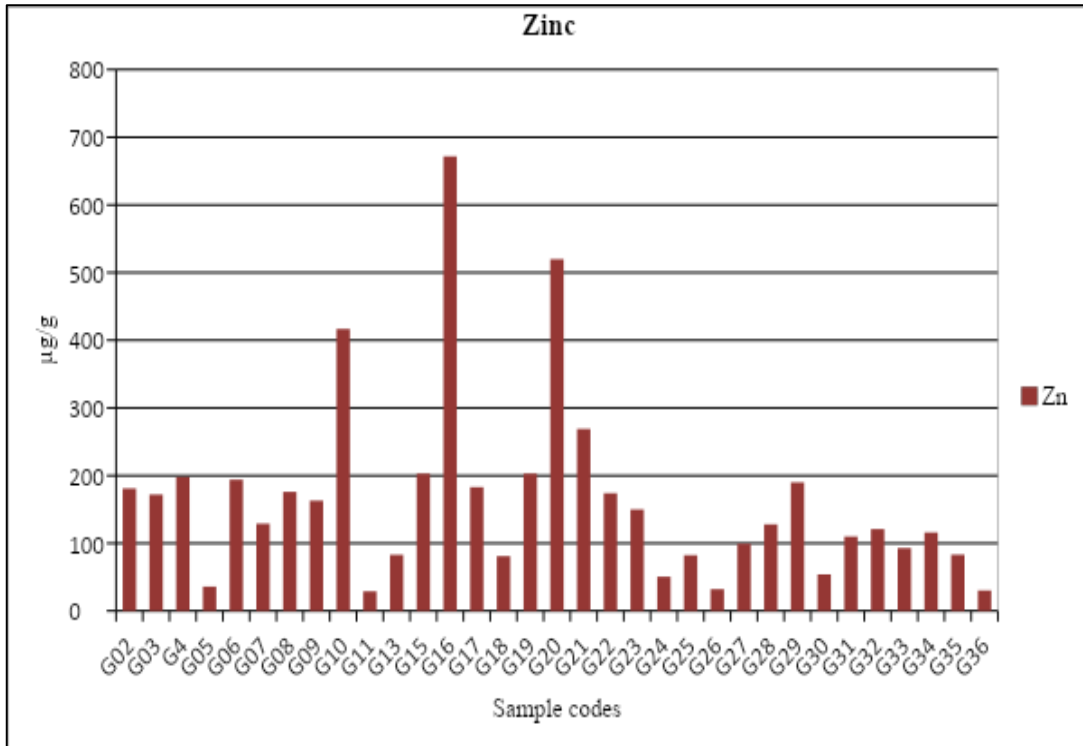


Figure 4- 6: Variation of concentrations of zinc

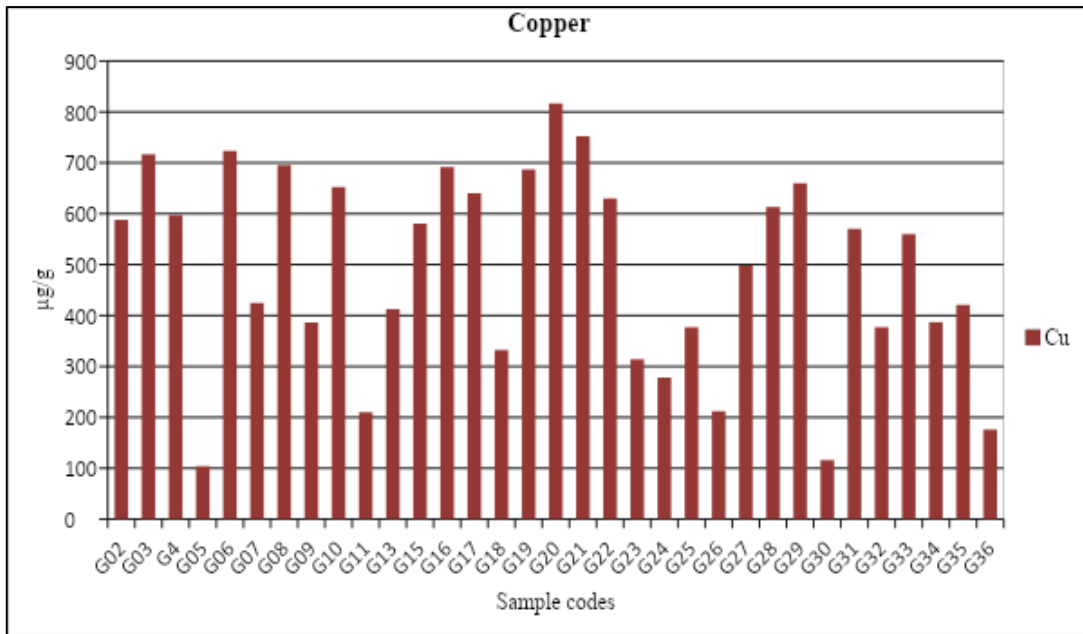


Figure 4- 7: Variation of concentrations of copper

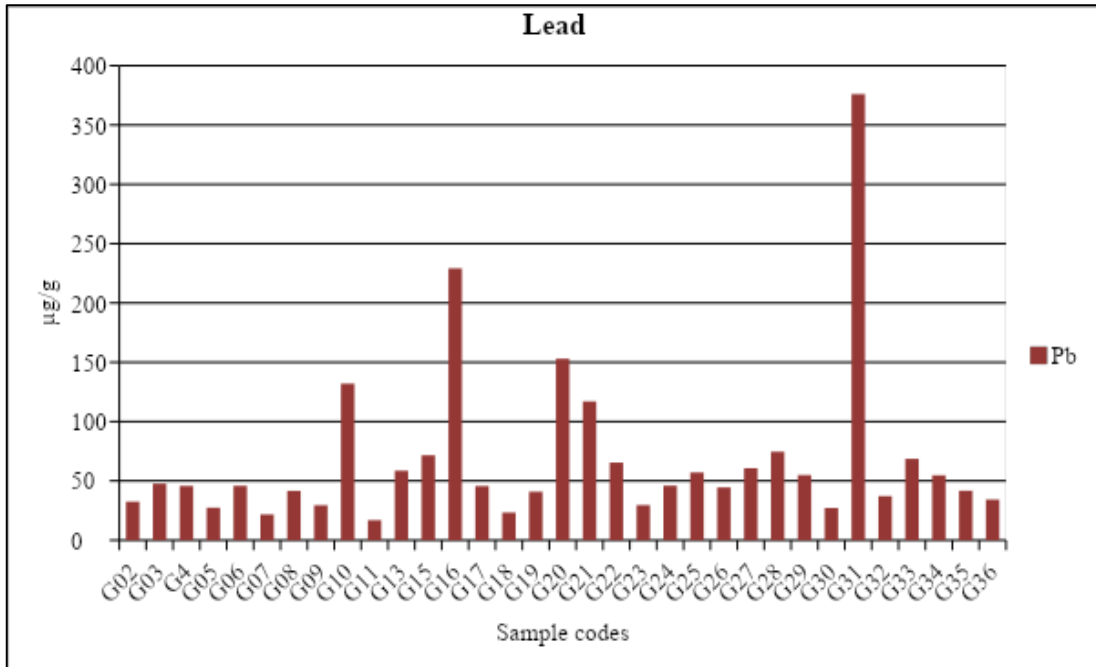


Figure 4- 8: Variation of concentrations of lead

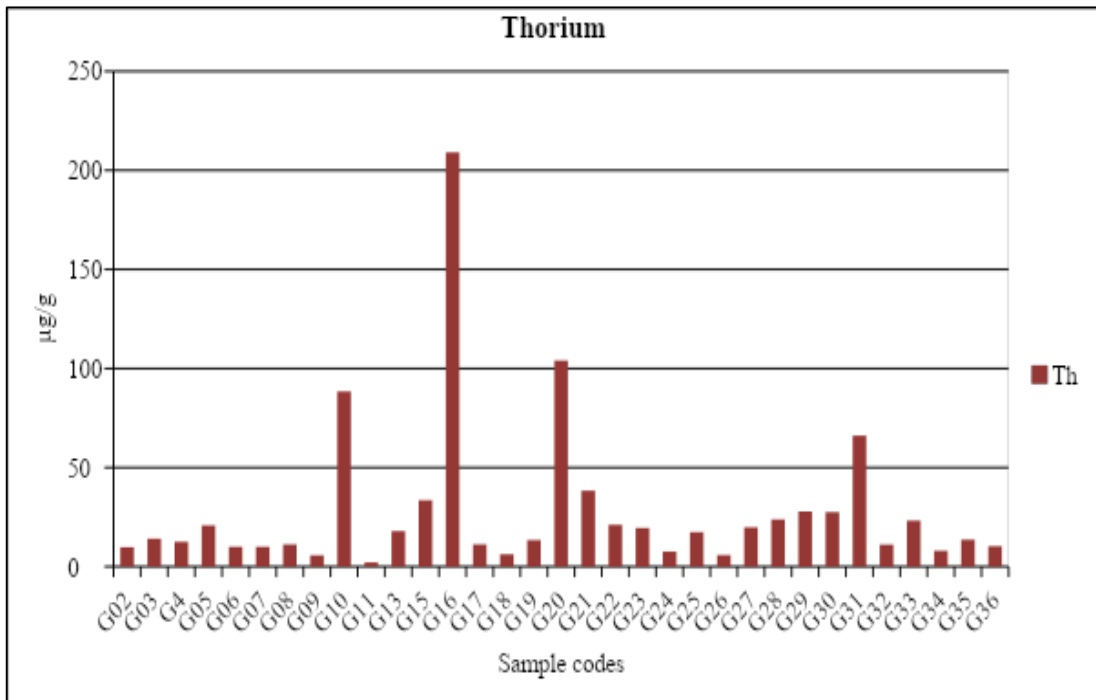


Figure 4- 9: Variation of concentrations of thorium-232

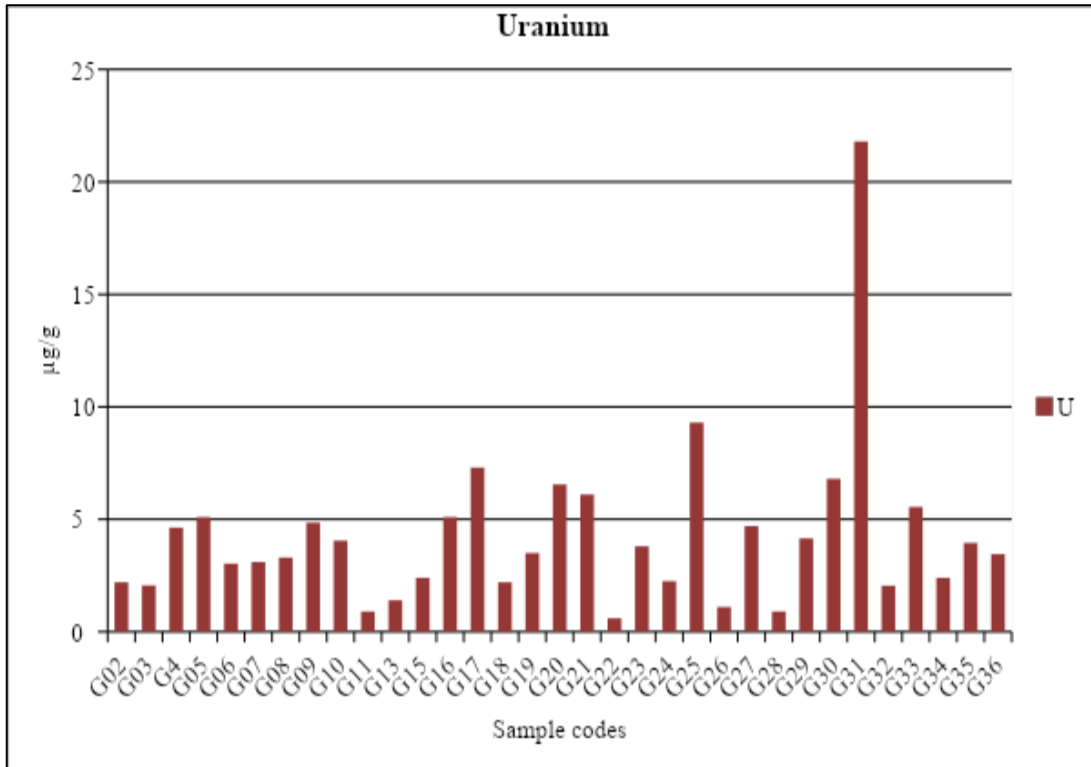


Figure 4- 10: Variation of concentrations of uranium-238

From the analysis, iron is the only element found to be in high concentrations. However, since economic viability of an ore is depended on other factors such as size, shape, depth of the ore below the surface, proximity of the ore to existing infrastructure, the price of the mineral and other factors such as labor cost, the grade of iron in this area can therefore not be exclusively determined to be economically viable.

The results of elemental analysis of all the samples are presented in Appendix I.

Table 4-3 shows the minimum economic viability of ores of the elements analyzed.

Table 4- 3: Minimum economic viability of ores of the elements analyzed (µg/g).

	K	Mn	Fe	Cu	Zn	Pb	Th	U
Maximum	37166	22933	289800	817	672	74.6	209	20.2
Minimum	236	89	1972	104	29	17	8.0	7.3
Minimum Economic Viability	50,000	23,000	250,000	10,000	50,000	50,000	10,000	10,000
Viability (EV/NEV)	NEV	NEV	EV	NEV	NEV	NEV	NEV	NEV

EV-Economically Viable, NEV- Not Economically Viable

(Source: A. Post, 1983; J. Warren, 2006)

4.5 Variation of the NORMs in the soils and rock samples

Figure 4-11 shows the HpGe Gamma Ray Spectrum of soils for the activity concentration measurements of lead-212, lead-214, bismuth-214, actinium-228 and potassium-40 nuclides for determination of the activity of Thorium-232, Uranium-238 and potassium-40.

Table 4-4 shows the results of measured activity values of thorium-232, uranium-238 and potassium-40 in soils.

Figure 4-12 shows the variation of uranium-238, thorium-232 and potassium-40 activities in the soil samples.

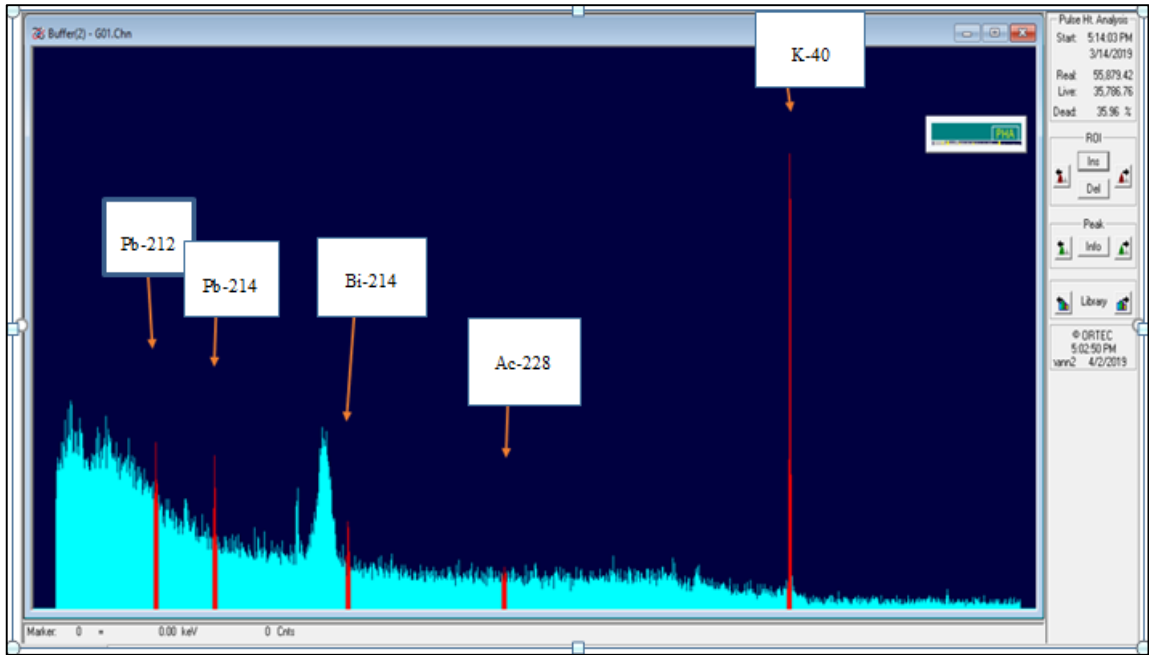


Figure 4- 11: HpGe Gamma Ray Spectrum of activity concentration of soils in the study area

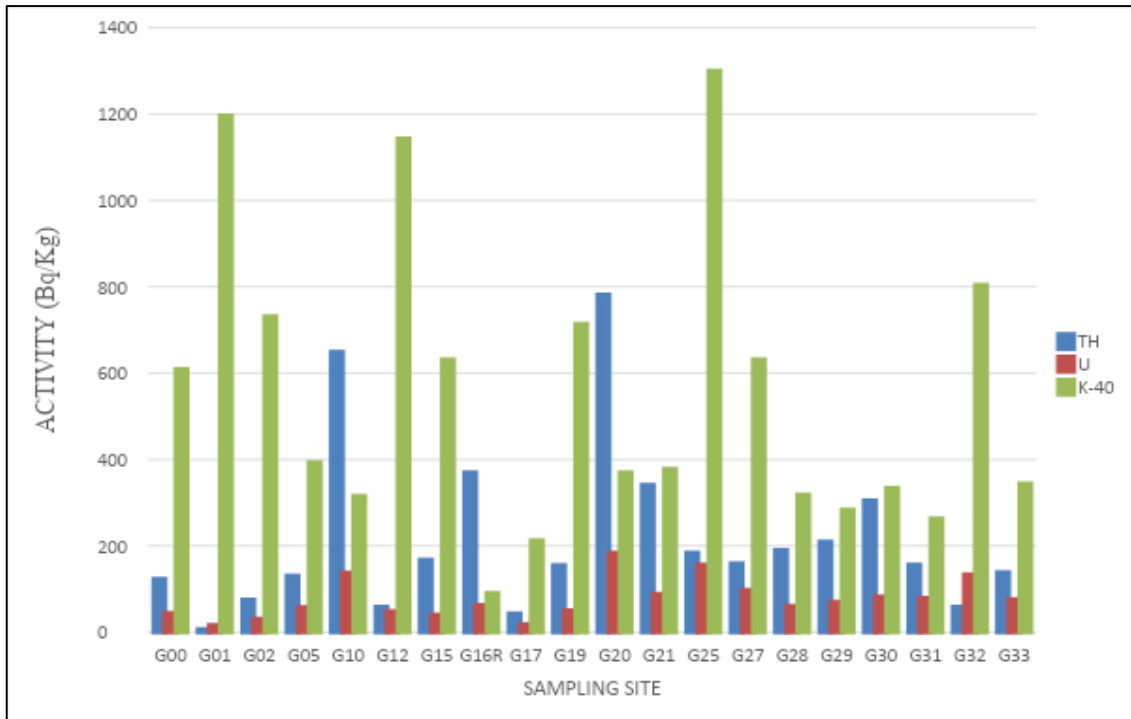


Figure 4- 12: Variation of uranium-238, thorium-232 and potassium-40 activities in the soil samples

Table 4- 4: Measured activity concentration of ²³²Th, ²³⁸U and ⁴⁰K in Bq/kg in soils; (n=1, x ±1δ)

SAMPLE SITE	thorium-232	uranium-238	potassium-40
G01	123 ± 18	43.3 ± 3.8	608 ± 31
G02	6.3 ± 5.0	16.5 ± 1.6	1196 ± 34
G03	74.5 ± 7.9	30.6 ± 5.2	731± 53
G05	130 ± 9.0	57.5±14	393±33
G10	648±31	138±2.1	315±38
G12	58.3±3.7	48.2±6.5	1143±49
G15	168±8.9	39.9±0.7	631±35
G16R	369±28	62.3±4.9	90.3±22
G17	42.7±3.3	17.7±10	212±28
G19	155±23	50.0±2.0	713±36
G20	782±39	183±20	369±40
G21	341±59	87.5±5.7	378±45
G25	183.9±15	156.0±13	1300±13
G27	159±19	97.4±3.3	631±40
G28	190±5.5	60.1±6.7	318±25
G29	209±6.4	69.7±7.4	284±30
G30	304±16	81.7±3.9	334±24
G31	156±16	78.7±2.3	263±19

G32	57.8±7.6	133±4.9	804±38
G33	139±7.2	75.6±1.2	343±25
Mean	215	76.3	553
Standard deviation	16	6.0	33
Maximum	782	183	1300
Minimum	6.3	16.5	90.3

In general, ^{40}K was found to be the leading contributor of the radiation exposure in the area of study, with a mean measured activity concentration of 553 Bq kg^{-1} , as compared to ^{232}Th and ^{238}U at 215 Bq kg^{-1} and 76 Bq kg^{-1} independently. The mean activity levels of ^{238}U , ^{40}K , and ^{232}Th , were all above UNSCEAR reported global mean of 35, 30 and 400 Bqkg^{-1} in that order (UNSCEAR, 2000).

The recorded values of potassium-40 and thorium-232 found in the study area are comparable to those found in soil samples of Malnichera Tean Garder in Sylhet District of Bangladesh. These values are however below the values reported in similar environments. The study done by Alamgir et al (2012) in Malnichera, to assess the natural radioactivity and accompanying dose rates in the soil samples determined the mean concentration values at 125.27 Bqkg^{-1} for ^{232}Th , 55.25 Bqkg^{-1} for ^{238}U and ^{40}K at 497.91 Bqkg^{-1} . Similar values were obtained by Sowmya et al. (2010) when they were analyzing the associated dose rates and natural radioactivity in samples of soils collected from South India, specifically Kalpakkam,. From the study, the highest mean activity level was recorded for ^{40}K at 607.0 Bqkg^{-1} , ^{238}U at 53 Bqkg^{-1} , and ^{232}Th 163 Bqkg^{-1} . However, Ademola et al. (2015) in a study to analyze the natural radioactivity and associated hazards in the soil samples around the gold mining area of Itagunmodi, a region located in south Western Nigeria, reported the mean activity levels for ^{238}U , ^{40}K , and ^{232}Th at 55 Bqkg^{-1} , 505 Bqkg^{-1} and 26 Bqkg^{-1} , respectively.

Figure 4-13 shows the relative abundance of the naturally occurring radionuclides in the measured soil samples. From the figure, ^{40}K was found to be the largest contributors to radionuclide at 65.5% followed by ^{232}Th at 25.8% and ^{238}U at 9.0%. These results can be attributed to the existence of potassium bearing minerals like micas and feldspars in the lithological profile of the study area (Mohammadi et al., 2006). thorium-232 and uranium-238 bearing minerals such as silicates, phosphates and hydroxides are responsible for the elevated levels of Thorium-232 (Bella et al 1997).

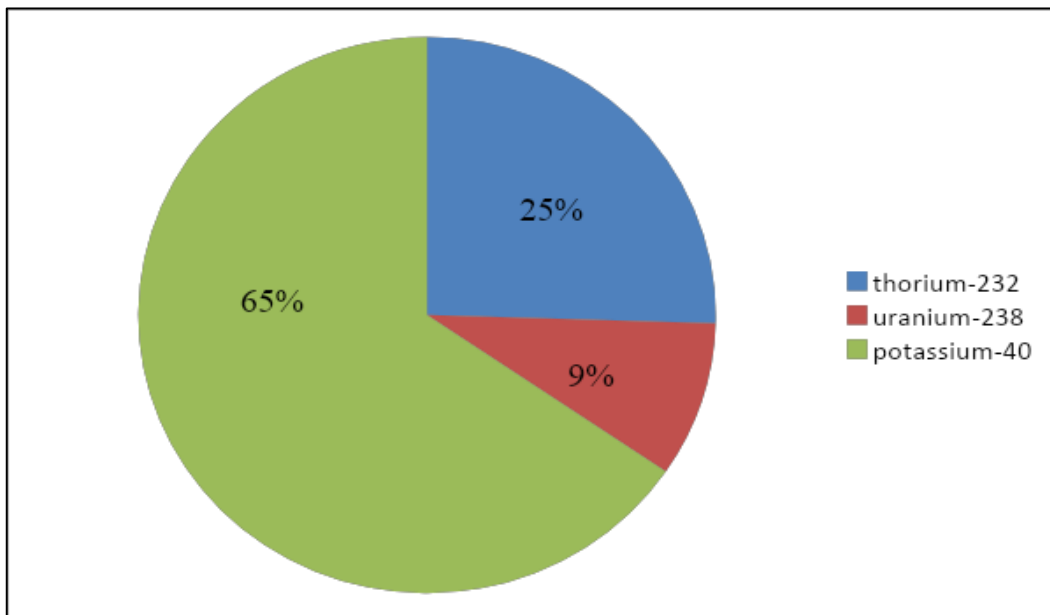


Figure 4- 13: Relative abundance of the naturally occurring radionuclides in the measured soil samples

4.6 Results of statistical data analysis of radioactivity

Table 4-5 and Figures 4-14 to 4-16 show the results of correlation and analysis of the linear regression of the data of the measured activity concentrations of thorium-232 and uranium-238 and potassium-40.

Table 4- 5: Correlation of uranium-238, thorium-232 and potassium-40 activities

	<i>Thorium-232</i>	<i>Uranium-238</i>	<i>Potassium-40</i>
Thorium-232	1		
Uranium-238	0.683981	1	
Potassium-40	-0.42481	0.1696	1

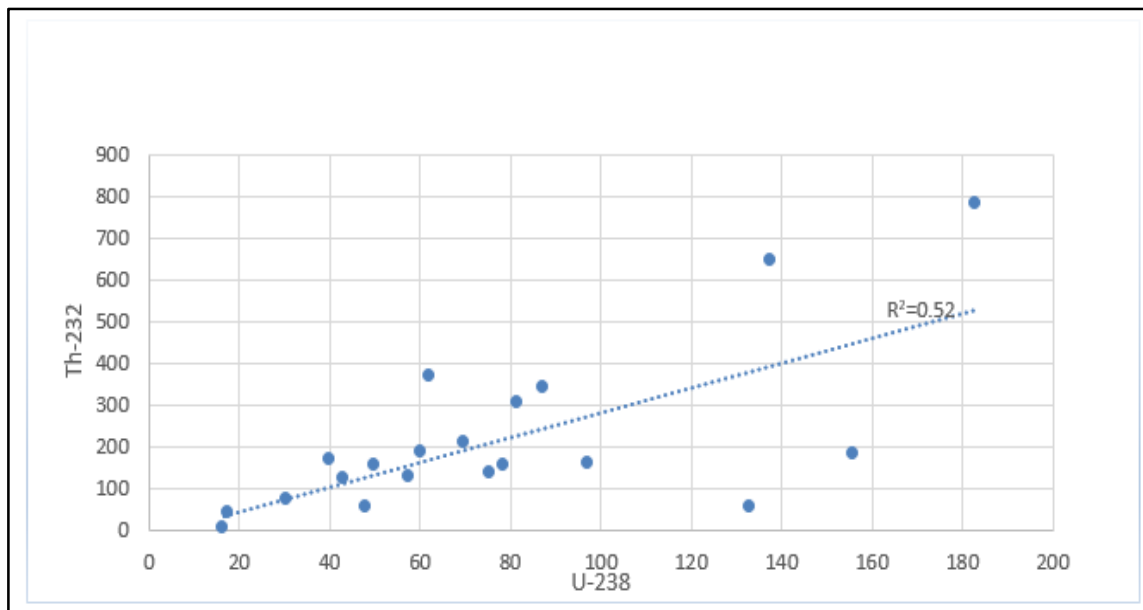


Figure 4- 14: Correlation of thorium-232 with uranium -238

For uranium-238 and thorium-232 radionuclides, there was a linear relationship which exhibited a positive coefficient of $R^2 = 0.52$ (Fig. 4-15). This suggests that uranium -238 and thorium-232 are affected by the same local geological and mineralization factors in the study area. Similar findings have also been reported by the International Atomic Energy Agency (IAEA, 2014) showing that uranium -238 and thorium-232 occur together in carbonitic rocks, alkaline rocks, granites and peralkaline rocks. In addition, Vasudeva (1989) also found out that both thorium-232 and uranium M-238 occur in the same mineralogical setting with the mineral sphene being specifically common and alanine occurring only in trace amounts. These results are similar to the findings of the results of

Miah et al, which recorded significant variation in occurrence of uranium -238 and thorium-232 when conducting a study to find out the natural radioactivity levels in the soil samples and the associated dose rates at Malnichera Tea Garden in Sylhet, Bangladesh. The study attributed this difference to chemical changes of the constituent elements in the soils (Miah et. al, 2012).

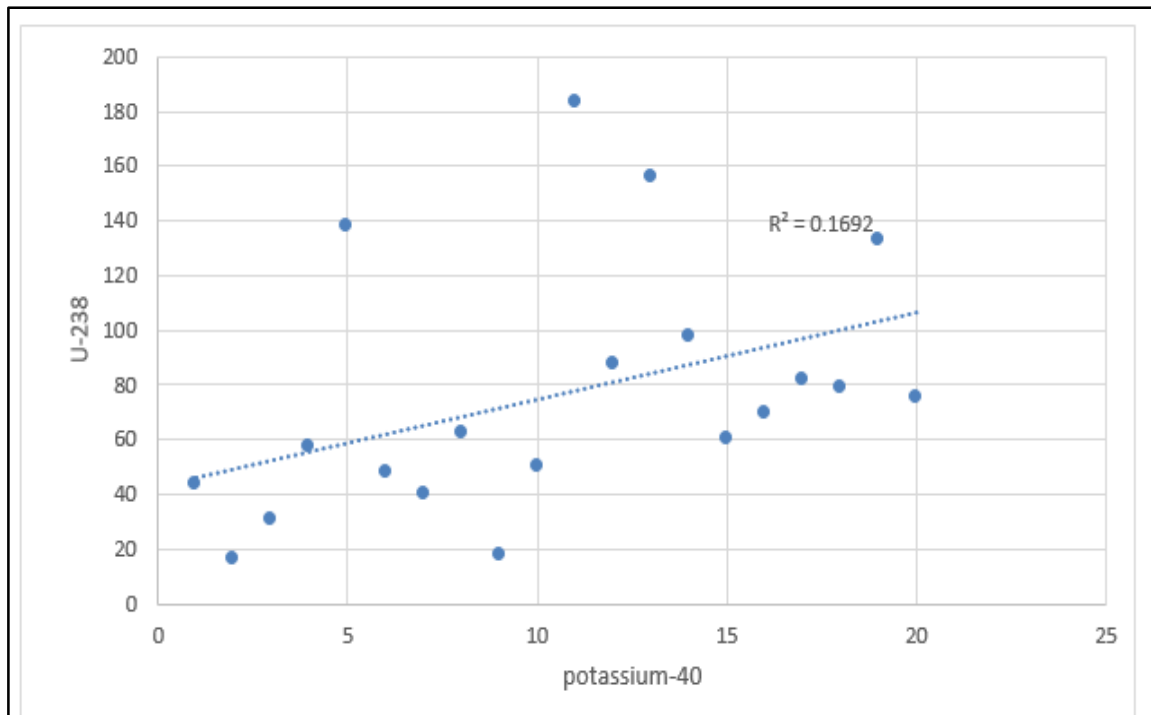


Figure 4- 15: Correlation of uranium-238 and potassium-40

Figure 4-15 shows correlation of the variation of the activity between uranium -238 and potassium-40.

For uranium-238 and potassium-40 radionuclides, there was a weak positive correlation coefficient of $R^2 = 0.1692$ in the study area. This is because potassium has low kinesis and therefore, its concentration in soil reflects the disparities occurring within the host geological material. In addition, the distribution of potassium-40 and uranium-238 is dependent on the pH, levels of organic matter and levels of occurrence of clay minerals from soils (Ion, 2014). Similar trends were also noted by Abusini et. al (2007) when conducting a study to determine uranium -238, thorium-232 and potassium-40 activity levels in soil cores of the anomaly at Araba valley, Jordan. (Samreh et al. 2014). The study

found a significant variation in activity between uranium -238 and potassium-40 when measuring their concentration levels in West Bank.

Figure 4-16 shows correlation of the variation of the activity between thorium -232 and potassium-40.

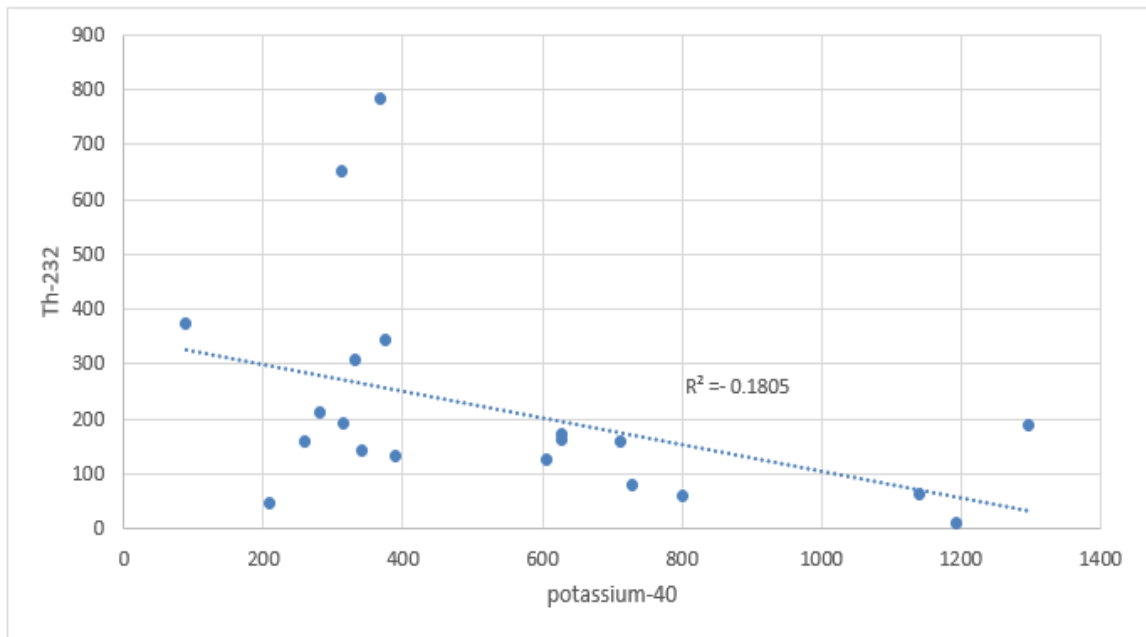


Figure 4- 16: Correlation of thorium-232 and potassium-40

For thorium-232 and potassium-40 radionuclides, there is a negative correlation coefficient of $R^2 = -0.1805$. This inverse relationship suggests that the occurrence of the two radionuclides do not depend on the same physical and geochemical factors. Although thorium-232 and potassium have low mobility with their concentrations depending on the acidity, levels of biological matter as well as the presence or absence of clay minerals in these soils (Ion, 2014), the mobility of these radionuclides is largely dependent on the pH. Whereas potassium-40 mobility is high in more acidic environment, ^{232}Th is more mobile in basic environments (Fernandes, 2017).

4.7 Radiation Hazard Indices

The activity caused by Radium (Ra_{eq}), internal (H_{in}) hazard index, Gamma index (I_{γ}), external hazard index (H_{ex}), absorbed dose rate (DR) and annual effective dose (E) were

utilized to estimate the indices of the hazards caused by the radiation levels in the study area. The indices were computed from the mean measured values of earlier obtained activity concentration levels of ^{238}U , ^{40}K and ^{232}Th . Table 4-6 shows a summary of obtained values of the radiation hazard indices of these radionuclides.

Table 4- 6: Summary of mean radiation hazard indices

Descriptive statistics	R_{eq} (Bq kg⁻¹)	I_{yr}	H_{ex}	H_{in}	Dr	E
Mean	425.91	3.03	1.15	1.36	198.50	0.48
Stdev	287.97	2.50	0.95	1.08	164.30	0.20
Max	1401.00	80.25	3.78	4.28	651.55	1.60
Min	32.49	0.23	0.09	0.13	15.11	0.04
Recommended	<350	<1	<1	<1	<43	<0.5

In this study, Radium equivalent (R_{eq}) was used as a factor for determining the radiation hazards, to overcome the inconsistencies of most natural radionuclides in a material. This also takes into considerations the assumption that equal gamma ray dosage is produced by 259 Bq kg⁻¹ of ^{232}Th , 370 Bq kg⁻¹ of ^{226}Ra and 4810 Bq kg⁻¹ of ^{40}K (Taiwo A.O. *et al.* 2014).

The values of the radium equivalent, were determined to be between 32.49 to 1401 Bq kg⁻¹ and the mean value of 425.91Bq kg⁻¹. All these values exceed the world average of 160 Bqkg⁻¹, and area above the global recommended limit of 350.00 Bq kg⁻¹ according to the report from the UNSCEAR, (2000).

The radiation index (I_{yr}) due to gamma, is used as a factor of measuring materials for any potential radiation health effects. The upper limit obtained for this value is 80.25 while the

lower limit is 0.23. The average gamma radiation index obtained is 3.03 and exceeds the average recommended dose levels, which should be less than unity (Samreh et al 2014).

Also, external (H_{ex}) and internal (H_{in}) hazard indices of this study were used to assess the levels of risks of internal and external exposures. The standard criterion is that values of up to unity are considered acceptable.

In this study, maximum obtained values of H_{ex} and H_{in} as 3.78 and 4.28 respectively and the minimum obtained values of H_{ex} and H_{in} were 0.09 and 0.13 respectively. The mean for H_{ex} and H_{in} was 1.15 and 1.36 respectively. Since the average values are greater than one, this gives an indication that the radionuclides present a significant hazard to the members of the public and the environment of Cheptais area (Table 4-6)

The absorbed dose rates (DR) cause by gamma radiations in air, measured at an assumed level of 1 m above the ground, were also measured and estimated. This was done with the assumption that ^{226}Ra , ^{232}Th and ^{40}K are evenly distributed. The other assumption is that the contribution of other radionuclides to the radioactivity of the area is not significant enough to cause a meaningful contribution to the total ambient background dose rates of the study area. The obtained values ranged between 15.11 nGy/h and 651.55 nGy/h in the samples, with a mean value of 198.51 nGy/h, which is higher than the ICRP recommended value of less than 43 nGy/h. These values were further used to compute the annual effective dose (E), with an assumption of outdoor occupancy factor of 0.4 (Mustapha et al. 1999). The mean value of 0.48 mSv/y was obtained which is below the global mean annual effective dose, 0.5 mSv yr^{-1} , an indication that the annual effective dose does not pose significant risks to the public and environment.

CHAPTER 5: CONCLUSION AND RECOMMENDATIONS

5.1 Conclusion

In general, the major elemental constituents were found to be Fe (0.2-28.98) %, K (0.024 – 3.72) % and Mn (0.009 – 2.3) %. Other constituents such as Cu (0.01-0.08) %, Zn (0.003-0.07) % and Pb (0.002-0.037) % have concentration values of less than 0.1%. Although Th (0.00009-0.021 %) has concentrations that are lower than 0.03 %, these concentrations are still considered significant in comparison with the world average which ranges between 0.0008 %-0.0012 % for uncontaminated soils. For uranium, the global average ranges between 0.03%-1.2 percent. The results of uranium in the soil samples in Cheptais region (0.00007-0.002 %) are within that of the global average.

The study has also determined the radionuclide content of naturally occurring radionuclides in the soils around Cheptais region and their distribution patterns. ^{40}K was found to be the radionuclide with the highest contribution of background radiation accounting for 65.5% followed by ^{232}Th at 25.8% and ^{238}U at 9.0%. The radionuclide activity concentrations, gamma absorbed dose rates and annual effective dose rates were measured and established to be all above the world mean values. However, the effective dose rate was less than the recommended ICRP limits. Furthermore, the radiometric surveys measurements established that the highest readings recorded in the area were located approximately midway of the sampling area towards the South East in the fourth quadrant and constitute less than 15% of the study area.

The results of the statistical data analysis indicate a strong correlation between the three radionuclides in the area of the study. There is a positive correlation between uranium-238 and potassium-40, and between uranium -238 and thorium-232. However, there was a negative correlation between thorium-232 and potassium-40. There was also a significant difference in the variation of activity levels between each of the naturally occurring radionuclides.

Generally, the external radiation hazard index from all soil samples analyzed was above one. The radium equivalent was observed to be above the 370Bqkg^{-1} global average values.

The area therefore, has a high background radiation dose levels considered hazardous to the residents.

5.2 Recommendations

This study, therefore, recommends the following:

- 1) For detailed studies, specifically on ^{232}Th distributions in the wide area of Cheptais, for a more comprehensive quantification of this radionuclide in the delineated areas from aerial radiometric surveys.
- 2) Continuous and periodic monitoring of background radioactivity, ambient absorbed and annual effective dose rates in soil, rock, and building materials
- 3) For NORMS radioactivity measurements in water sources; rivers, boreholes, etc. for radio-ecological assessments.

REFERENCES

- Adel G.E.A., 2004. Estimation of radiation hazard indices from sedimentary rocks in Upper Egypt. *Journal of Applied Radiation and Isotopes Vol. 60: pp 111-114.*
- Abusini et. al, 2007. Determination of uranium-238, Thorium-232 and potassium activity concentrations in soil cores in Araba valley, Jordan, *Radiation Protection Dosimetry, Volume 128, Issue 2.* 214-216.
- Ademola et al., 2014. Determination of natural radioactivity and hazard in soil samples in and around gold mining area in Itagunmodi, South-Western Nigeria. Department of Physical Sciences, Bells University of Technology, PMB 1015, Sango-Ota, Ogun State, Nigeria. *Journal of Radiation Research and Applied Sciences* 7:3, 249-255
- AEA, 1958. Aerial Radiometric Survey of a Probable Uranium-238 Province in Kenya, Nairobi
- Agola, J.O., 2006 Assessment of Natural Radiation Levels in Olkaria Geothermal Area. MSc Thesis, University of Nairobi. pp 49-51, 71.
- Ajlouni et al., 2009. A very high natural radiation area in Afra hot springs. *Radiation Protection. Dosimetry* 133(2):
- Alamgir M. et. al, 2012. Natural Radioactivity and Associated Dose Rates in Soil Samples of Malnichera Tea Garden in Sylhet District of Bangladesh, *Journal of Nuclear and Particle Physics, Volume 2(6):* 147-152
- Bella, S., et al., 1997. Natural radioactivity in a volcanic island: Ustica, Southern Italy, *Applied Radiation and Isotopes, Volume 48, Issue 2, February 1997,* pp 287-293.
- BGS (2004): *The economic importance of minerals in the UK.* Keyworth, Nottingham.
- Bomuhangi et al, 2016. Local communities' perceptions of climate variability in the Mt. Elgon region, eastern Uganda. *Cogent Environmental Science* (2016), 2:1
- Bubois C. & Walsh J., 2007, Minerals of Kenya- Geological Survey of Kenya: Mines and Geology Department, Nairobi, Kenya.
- Cox, P.A, 1995. The elements on Earth- inorganic chemistry in the environment. Oxford University Press, New York.

- Cullen, T. L., Penna Franca, E., 1975, Proceedings of International Symposium on Areas of High Natural Radioactivity, Academia Brasileria De Ciencias, Rio de Janciro, Brazil, pp. 49-64.
- EPRA, 2015. Least Cost Power Development Plan, 2015. Nairobi.
- Fernandes, T. 2017: Geochemical behaviour of Uranium-238 and Thorium-232 in the Waste of a Uranium-238 conversion facility, PhD thesis, Autonomous University of Barcelona, pp 49-51, 71.
- Garnie-Laplace et. al., 2010. Natural Uranium and the Environment. Radionuclide Fact Sheet. K. Beaugelin-Seiller, ISNR, Paris
- Gilmore G.& Hemingway, J., 1995. Practical Gamma-Ray Spectrometry, *John Wiley and Sons, Chichester*,
- Heuer, D., et al., 2014. Towards the Thorium-232 fuel cycle with molten salt fast reactors, *Annals of Nuclear Energy, Vol. 64, pp. 421-429*
- Ibrahim et al, 1993. Measurement of radioactivity levels in soil in the Nile Delta and middle Egypt. Central Laboratory for Environmental Radiation Measurements, Intercomparison and Training, Atomic Energy Authority of Egypt
- ICRP. 1993. Protection against Radon-222 at Home and at Work. *ICRP Publication 65. Ann. ICRP 23 (2)*.
- Isinkaye et al., 2018. Evaluation of radiological hazards due to natural radioactivity in bituminous soils from tar-sand belt of southwest Nigeria using HpGe-Detector, *International Journal of Radiation Research, Volume 6, pp 351-362*
- IAEA, 2014. International Symposium on Uranium-238 Raw Material for Nuclear Energy (URAM 2014) 23-27 June 2014, Vienna, Austria
- Ion, A., 2014. Uranium, Thorium, Potassium and Cesium in the surface layers of soils from Lehliu area, Romania, EGU General Assembly.
- Vasudeva, R. et al., 1989. Prospecting for uranium in carbonate rocks of 19 Vempalli formation, Department of Atomic Energy. Proceedings of International Symposium on URANIUM-238 Technology, Bhabha Atomic Research Centre, Trombay, Bombay, 400 085
- Kabata Pendias & Pendias (2001). Trace Elements in Soils and Plants. CRC Press LLC, 2000 N.W. Corporate Blvd, Boca Raton, Florida 33431

- Klepper, M. R. & Wyant, D.G. 1957. Notes on the Geology of Uranium-238, Issue 1046. USGS, VA, USA
- Knoll, G.F., 2000. Radiation Detection and Measurement. 4th Edition, John Wiley & Sons, Inc., New York.
- Lakkundi, T., 2012. Geology and Mineral Resources of Kenya with Special Emphasis on Minerals around Mombasa, Patel Mining. Maputo.
- Lin, Y., Chen, C., & Lin, P., 1996. Natural background radiation dose assessment in Taiwan, *Environment International, Volume 22, Supplement 1, 1996*.
- Maina, D. M., Kinyua A. M., Nderitu S. K., Agola J. O. and Mangala M. J. (2002). Indoor Radon (²²²Rn) Levels in Coastal and Rift Valley Regions of Kenya. *International Atomic Energy Agency (IAEA), IAEA-CN-91/56, 401 - 405*.
- Mangala, J. M. (1987) A multi-channel X-ray fluorescence analyses of fluorspar ore and rock from Mrima hill, Kenya. M.Sc. thesis, University of Nairobi.
- McCall, G. J. H. (1958) Geology of the Gwasi area, Ministry of Commerce and Industry, Geology survey of Kenya, Dept. No. 45
- Miah et. al, 2012: Natural Radioactivity and Associated Dose Rates in Soil Samples of Malnichera Tea Garden in Sylhet District of Bangladesh, *Journal of Nuclear and Particle Physics, Volume 2(6): pp 147-152*
- Mines and Geology Department, 2010. 'Geohazard Mapping and Assessment of the Kapkirongo Area of Mt. Elgon.' Ministry of Environmental and Mineral Resources, Nairobi.
- Mohammadi, S. et al., 2006. Adaptive response of blood lymphocytes of inhabitants residing in high background radiation areas of Ramsar- Micronuclei, Apoptosis and Comet Assays. *Journal of radiation research. Volume 47. Pp 279-85*.
- Mustapha, A.O., 1999. Assessment of Human Exposures to Natural Sources of Radiation in Kenya. Ph.D. Thesis, University of Nairobi.
- Nash, J. T., 2010. Volcanogenic Uranium-238 deposits—Geology, geochemical processes, and criteria for resource assessment: *U.S. Geological Survey Open-File Report 2010-1001, 99 p*.
- Nema, P.K., 2010: Application of Accelerators for Nuclear Systems: Accelerator Driven System (ADS), MD&PD Division, BARC, Trombay, Mumbai 400 085, India.

- Otwoma, D., 2012. An investigation of the Radioecology of the Carbonatite deposits in the Homa Mountain region in South Nyanza, Kenya, PhD Thesis, University of Nairobi.
- Paschoa, A.S. and Steinhäusler F., 2010. Technologically Enhanced Natural Radiation. Vol. 17, Elsevier.
- Patel, J.P., 1991. Environmental Radiation Survey of the area of High Natural Radioactivity of Mrima Hill of Kenya, *Discovery and Innovation*, 3(3): 31-35
- Pulfrey, W. & Walsh, J. (1969): The Geology and Mineral Resources of Kenya, Geological Survey of Kenya, Ministry of Natural Resources, Bulletin No. 9, Nairobi.
- Samreh et al. (2014). Measurement of Activity Concentration Levels of Radionuclides in Soil Samples Collected from Bethlehem Province, Westbank, Palestine. *Turkish Journal of Engineering and Environmental Sciences*, Volume 38. Pp 113-125.
- Selvasekarapandian, S. et al., 1999. Gamma radiation dose from radionuclides in soil samples of Udagamandalam (Ooty) in India. *Radiation Protection Dosimetry* 82 (3). Pp225-227.
- Shenber, M.A., 1997. Measurement of natural radioactivity levels in soils in Tripoli. *Journal of Applied Radiation and Isotopes*. Volume 48. pp. 147-148
- Sohrabi, M., 1995. Recent radiological studies of high level natural radiation areas of Ramsar, Iran, International Conference of high levels of natural radiation, Ramsar, Proceeding Series, p618. 3-7 Nov, 1990.
- Sroor, A. 2002. Environmental Pollutant Isotope Measurements and Natural Radioactivity Assessment for North Tushki Area, South Western Desert, Egypt. *Applied Radiation Isotopes*, Vol. 57, pp. 427-436
- Sunta, C. M., 1993. A review of the studies of high background areas of the S-W coast of India. Proceeding Series 618. IAEA, Vienna.
- Taiwo A.O. et al. (2014). Determination of external and internal hazard indices from natural occurring radionuclide around a superphosphate fertilizer factory in Nigeria. MSc Thesis, Department of Physics, Ahmadu Bello University Zaria, Nigeria
- Tsurikov, N., 2009. Uranium exploration-safety, environmental, social and regulatory considerations. Version 2. Calytrix Consulting Pvt. Ltd., Perth.

- UNSCEAR, 2000. Sources of ionizing radiation. Report to the General Assembly. (Vol.1).
United Nations Publications.
- UNSCEAR, 1993. Sources of ionizing radiation. Report to the General Assembly.
Supplement No. 46 (N48/46). United Nations Publications.
- UNSCEAR, 2012. Sources, Effects and Risks of Ionizing Radiation. Report to the General
Assembly. Supplement No. 46 (A/67/46). United Nations Publications.
- USGS, 2019. 2015 Minerals Yearbook, Kenya (Advanced Release), U.S. Department of
the Interior and U.S Geological Survey, 12201 Sunrise Valley Drive Reston, VA
20192, USA
- Velzen, L. 2015. Environmental remediation and restoration of contaminates nuclear and
norm sites, NRG Nuclear Research and consultancy, Woodhead Publishing, The
Netherlands
- Wei, L. (1980) Health surveys in high background radiation areas in China, Journal of
Science Volume 209(4459). pp 877-880 WNA (2017).
- WNA (2017). World Nuclear Performance report, August 2017. London.

APPENDIX I: Elemental concentrations in µg/g in the soil samples of Cheptais area

	K	Mn	Fe	Cu	Zn	Pb	Th	U
G01	16901±734	2217±132	206700±25337	692±73	203±23	69.3±7.0	10.3±3.0	<5.0
G02	26900±1348	4417±205	127600±5533	588±45	181±18	32.5±7.0	9.80±3.0	<5.0
G03	12400±1700	6420±415	193933±10566	717±47	172± 19	47.7±9.0	14.1±3.0	<5.0
G4	21700±1100	8000±407	174133±7766	597±35	198±16	45.8±11.0	12.5±3.0	<5.0
G05	14915±774	768±126	23400±2933	104±18	36±8.0	27.4±6.0	20.8±4.0	<5.0
G06	37166±2866	4460±250	137933±5667	723±41	194±17	45.9±10.0	10.0±3.0	<5.0
G07	14500±6233	3914±1550	114600±4436	425±169	129±54	<10	<6.3	<5.0
G08	16300±1041	5941±286	185200±8500	695±45	176±17	41.6±8.0	11.2±3.0	<5.0
G09	19300±1111	4997±199	113200±4066	386±29	163±15	29.5±6.0	<6.3	<5.0
G10	11286±1857	17666±1200	228900±15066	652±51	417±33	132±14	88.4±7.0	<5.0
G11	15600±1390	7880±517	195150±12633	210±58	210±20	53.9±10	16.9±4.0	<5.0
G13	16966±1533	2587±159	78500±3233	413±26	83±11	58.6±8.0	17.9±3.0	<5.0
G15	21000±1733	7486±357	149733±6233	581±34	203±18	71.6±9.0	33.5±4.0	<5.0
G16	8792±1375	22933±766	231933±7100	692±38	672±34	29.0±23.0	209±9.0	<5.0
G17	19600±2166	5990±298	178933±7566	640±37	183±17	45.7±9.0	11.2±3.0	7.3±2.0
G18	8243±617	2664±121	92500±3866	332±28	81±10	23.3±6.0	<6.3	<5.0
G19	25133±2166	5985±329	154033±7200	687±41	203±18	40.9±8.0	13.4±3.0	<5.0
G20	19700±2200	21550±950	289800±12500	817±52	520±37	53.0±14.0	24.0±6.0	<5.0
G21	14100±2000	13550±650	257300±12000	752±46	269±22	17±13	38.3±4.0	<5.0
G22	16333±1866	8270±455	183633±8900	630±41	174±15	65.4±11	21.1±3.0	<5.0

G23	12350±1224	499±51	39950±1650	314±20	150±18	29.6±5	19.5±4.0	<5.0
G24	20300±1142	422±42	35800±1676	278±27	50.6±8	46±8	<6.3	<5.0
G25	19933±1900	1029±88	55033±2733	377±26	82.4±10	57.1±8	17.4±2.0	9.3±2.5
G26	73600±725	890±40	6406±2140	212±43	32.2±8	44.5±13	<6.3	<5.0
G27	15033±1733	3798±221	118900±5633	498±38	199.3±9	60.7±9	19.8±3.2	<5.0
G28	10346±1323	5633±288	245133±9533	613±40	128±16	74.6±12	23.8±3.0	<5.0
G29	12750±1143	8978±352	225650±7833	660±33	190±14	54.9±9	27.8±8.0	<5.0
G30	236±36	983±34	22600±700	116±7	54±5	27.2±7	<6.3	<5.0
G31	7302±1355	4664±294	190200±9700	570±37	110±14	66.1±9	21.8±4.0	<5.0
G32	25450±1920	2117±145	64400±3000	377±23	121±12	37.2±7	11.1±3.0	<5.0
G33	10068±1112	2299±149	155233±5800	560±31	92.9±12	68.6±9	23.2±3.0	<5.0
G34	14400±1566	1237±99	65800±3200	387±26	116±12	54.7±7	8.0±2.0	<5.0
G35	26450±1372	765±57	39700±1819	421±33	83.2±10	41.7±8	13.6±2.0	<5.0
G36	16541±1229	214±10	9029±193	176±64	30.3±12	34.3±12	10.3±3.0	<5.0
RG01	1708±674	205±35	1972±129	367±24	64.6±9.7	34.8±7.7	<6.3	<5.0
RG07	16855±1582	2922±175	85600±3266	745±40	183±18	39.1±12	<6.3	19.4±5.0
RG14	27866±2533	215±37	2426±158	416±28	37.5±8	30.9±10	<6.3	18.3±4.8
RG16	2132±1287	6438±313	45733±1800	625±37	239±18	17±16	18.0±4.0	18.2±6.0
RG14	15977±1091	1555±201	45979±5320	589±105	192±31	32.9±8	<6.3	<5.0
RG25	7054±1933	312±107	4722±1376	333±81	33.3±11	51.6±16	<6.3	18.7±3.8
RG38	31400±2400	2625±162	87600±3333	705±39.0	162±16.0	41.0±10.0	>	20.2±5.8
AV.	15498±8527	5062	116457±82252	500±192	158±129	64.8±18.45	26.3±9.1	15.9±5.2
STDEV	8527	5491	82252	192	129	18.45	9.1	5.2

UPPER	37166	22933	289800	817	672	74.6	209	20.2
LOWER	236	89	1972	104	29	17	8.0	7.3